Journal of Membrane Science 658 (2022) 120740

Contents lists available at ScienceDirect

Journal of Membrane Science

journal homepage: www.elsevier.com/locate/memsci

Atomic layer deposition for membrane modification, functionalization and preparation: A review

Sen Xiong, Xiaofeng Qian, Zhaoxiang Zhong, Yong Wang *

State Key Laboratory of Materials-Oriented Chemical Engineering, College of Chemical Engineering, Nanjing Tech University, Nanjing, 211816, PR China

ARTICLE INFO

Keywords:
Atomic layer deposition
Membrane functionalization
Molecular layer deposition
Surface modification
Trade-off effect

ABSTRACT

Membrane separation is playing an increasingly important role in providing clean water and other resources to our thirsty globe. In addition to preparation of new membranes, modification and functionalization to existing membranes are frequently desired to maximize their performance. Among different strategies, the newly emerged atomic layer deposition (ALD) is distinguished for its universality in upgrading of almost all types of membranes independent of membrane structure and chemistry, as well as its striking capability of simultaneously enhancing selectivity and permeability. ALD is based on alternative reactions between gaseous precursors on solid surfaces including pore walls, and it deposits uniform and defect-free, angstrom-scale thin coatings conformally along the substrate surface. In this Review, we first discuss the basic principles of ALD and the early history of utilizing ALD to modify inorganic membranes for gas separation, and then analyze the advantages of applying ALD to upgrade membranes for water purification and gas separation. By directly ALD depositing metal oxides onto membrane surface, the hydrophilicity, fouling resistance and other properties are evidently improved. The (photo)catalysis, adsorption, antibacterial property, tunable wettability and other new functions can be integrated into membrane separation by ALD. Alternatively, some inert polymeric membranes are first subjected to surface activation, which greatly facilitating ALD processes and lowering the threshold for ALD to break the trade-off effect. For inorganic membranes, ALD has also been used to adjust the pore sizes, or to establish new separation layers to enhance the selectivity. We highlight recent progresses in ALD of polymeric materials on inorganic and polymeric substrates, producing advanced membranes with new configurations. Utilization of ALD to prepare or to functionalize new membranes, innovative ALD devices and processes, which are essential for the mass production of ALD-upgraded membranes, are also discussed. We conclude this review by discussing further development, challenges, and limitations of ALD-enabled membrane modification, functionalization, and preparation. As ALD is originally designed for microelectronics, and is not known for long and for many in the membrane community, we expect this review to inspire further attentions and research efforts tackling urgent problems of membrane separation. Also, it may spark new wave of studies on ALD and other advanced deposition technology toward next-generation membranes.

1. Introduction

With the merit of low costs, low carbon footprints, easy operation, and strong adaptability, membrane separation has been widely used for decades to provide clean water and other resources to industries and our daily life [1–3]. The membrane is the core part of the whole separation system and determines the performance of the separation process. Demands on membranes are keeping increasing, and a multibillion-dollar market has already formed and is rapidly growing [4]. According to the chemical nature of the membrane-forming materials, membranes can be roughly divided into three main groups: inorganic membranes (e.g. ceramic membranes), polymeric membranes (e.g. polyvinylidene fluoride (PVDF), polysulfone (PSF), and polyamide (PA) membranes), and hybrid or composite membranes containing both polymeric and inorganic components (e.g. mixed-matrix membranes). Typically, membranes possess an asymmetric structure composed of a "dense" separation layer and a "loose" support layer [5]. Generally, the ultrathin separation layer has smaller pores, which reduces the mass transfer resistance and guarantees the high selectivity during separation processes. The support layer has high porosity and good mechanical strength, which supports the separation layer and further reduces the

* Corresponding author.
E-mail address: yongwang@njtech.edu.cn (Y. Wang).

https://doi.org/10.1016/j.memsci.2022.120740
Received 11 May 2022; Received in revised form 12 June 2022; Accepted 14 June 2022
Available online 17 June 2022

Nomenclature

Methods abbreviations

ALD	atomic layer deposition
AALD	atmospheric atomic layer deposition
CFD	computational fluid dynamics
CVD	chemical vapor deposition
EDS	energy dispersive spectroscopy
MLD	molecular layer deposition
PVD	physical vapor deposition
PEALD	plasma-enhanced ALD
SIS	sequential infiltration synthesis
SALD	spatial atomic layer deposition

Material abbreviations

AZO	aluminum-doped zinc oxide
AAO	anodized aluminum oxide
BSA	bovine serum albumin
CNTs	carbon nanotubes
DEZ	diethyl zinc
EG	ethylene glycol
GO	graphene oxide
h-BN	hexagonal polymorph boron nitride
HDPE	high-density polyethylene
LLC	lyotropic liquid crystal
MOFs	metal organic frameworks
MPD	*m*-phenylenediamine
NFAs	nanofibrous aerogels
PA	polyamide
PC	polycarbonate
PI	polyimide
PP	polypropylene
PS	polystyrene
PU	polyuria
PAM	polyazomethine
PES	polyethersulfone
PSF	polysulfone
PDA	polydopamine
PIMs	polymers of intrinsic microporosity
PET	polyethylene terephthalate
PVDF	polyvinylidene fluoride
PTFE	polytetrafluoroethylene
$Pd(hfac)_2$	palladium hexafluoroacetylacetonate
PEDOT	poly(3,4-ethylenedioxythiophene)
PS-*b*-P4VP	polystyrene-*block*-poly(4-vinylpyridine)
RhB	rhodamine B
SA	sodium alginate
TMA	trimethylaluminium
TMC	trimesoyl chloride
TDMAT	tetrakis(dimethylamido) titanium-(IV)
ZIFs	zeolitic imidazolate frameworks

Other abbreviations

MF	microfiltration
MWCO	molecular-weight cut-off
NF	nanofiltration
NPs	nanoparticles
PWF	pure water flux
PPHF	PP hollow-fiber
RO	reverse osmosis
R2R	roll-to-roll
SCCM	standard cubic centimeter per minute
TFC	thin-film composite
UF	ultrafiltration
WCA	water contact angle

transport resistance. The separation layer contacts feed solutions directly, thus its physical and chemical properties have decisive impacts on the separation process.

For separation layers, uniform pore size, high porosity, appropriate wettability and some other properties are pursued to achieve desired separation performance [6]. However, the separation layers of many membranes only possess parts of these properties; as a result, surface modification is frequently required [7]. Common surface modification strategies mainly include chemical grafting [8,9], physical coating [7,12], plasma activation [10,11], etc. These strategies are usually material-specific, and are dependent on the chemistry of the membranes to be modified. That is, one specific modification method is only applicable to certain membranes with desired chemical properties, and cannot be shared between different types of membranes. Moreover, these modification strategies are usually "wet" as they are based on or at least involved with reactions in liquid phases. Because of the surface tension of liquids and unmatched wettability, liquids may not completely access fine pores in membranes, thus leading to inhomogeneous modification. Excessive coating and deficient coating may occur to the membrane pores (Fig. 1a). Consequently, conventional modification methods are usually faced with challenges such as tedious processing, non-uniformity, insufficient efficiency, pore blocking, and effluent generation. Additionally, many membranes are prepared from low-surface-energy polymers (e.g. polypropylene (PP), polytetrafluoroethylene (PTFE), and PVDF), which are difficult to be modified by common methods. To overcome these problems, some "dry" deposition processes, such as chemical vapor deposition (CVD) [12,13], magnetron sputtering [14], and initiated chemical vapor deposition [15] are used for membrane modification. However, there are still some issues in these deposition methods. Firstly, these methods are hard to deposit conformal and uniform layers on substrates with complex structures, especially the highly porous separation membranes. Secondly, the thickness of the deposition layer is challenging to be precisely controlled, facing the risk of blocking some small pores in the membranes.

As an advanced gas-phase deposition method, atomic layer deposition (ALD) is a subclass of CVD and originates from two independent paths, namely "atomic layer epitaxy" and "molecular layering" [16,17]. Compared to other deposition processes such as CVD and physical vapor deposition (PVD), ALD is known as a self-limiting deposition process and shows obvious differences. PVD is a physical process and requires only one solid precursor. CVD and ALD are chemical deposition processes; at least two precursors (solid, liquid, or gas) are required to complete the deposition, and the precursors should be gasified and transported into the reaction chamber. In CVD, two precursors are simultaneously and continuously pulsed into the reaction chamber to conduct the deposition. In ALD, the precursors are sequentially pulsed in different steps. Comparing with other two deposition methods, ALD can deposit film with the highest quality but in a slower growth rate. Nevertheless, the substrate surface coverage of PVD, CVD, and ALD is 50%, 60–80%, and ~100%, respectively [18]. The ALD can even modify the pores in the substrates with high aspect ratio, which allows the deposition of uniform and conformal films on substrates with highly complex structures [19], thus it is considered as an ideal technology to construct continuous thin coatings for many applications. With the rising of microelectronic industries, demands for high-quality thin films keep increasing and drive the fast development of ALD [20]. In the past two decades, researchers and engineers have explored the potentials of ALD and extended its

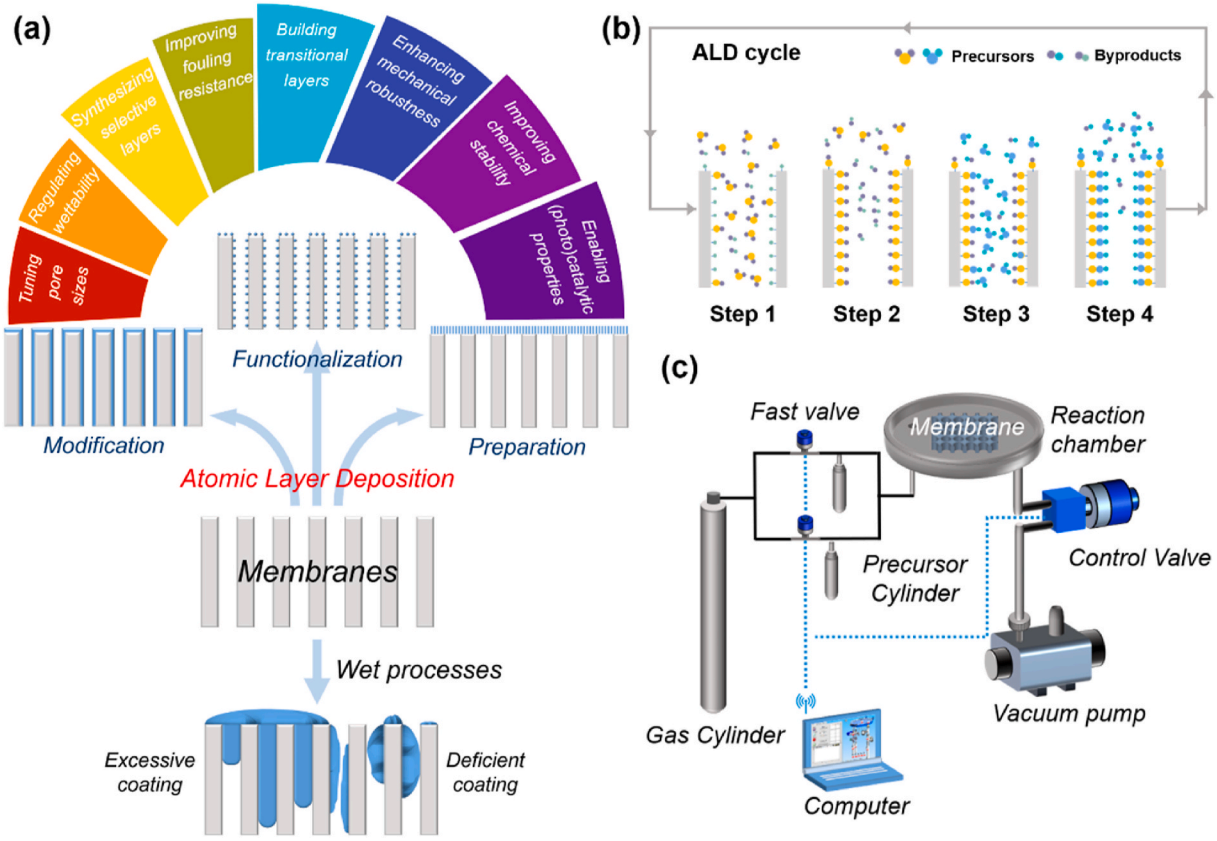

Fig. 1. Modification, functionalization, and preparation of membranes by ALD. (a) Comparison of ALD and wet processes in the modification and functionalization of membranes, and effects of ALD in the modification and functionalization of membranes; (b) Diagram of a typical ALD process for membrane modification. Step 1: precursor A pulse; Step 2: inert gas purge; Step 3: precursor B pulse; Step 4: inert gas purge. The exposure step is an optional step, which can be added between the pulse and purge steps; (c) Diagram of a typical ALD device working in the temporal mode.

applications into energy storage, batteries, solar cells, nanostructure fabrication, catalysts and so on [21–25]. A typical ALD process generally contains four steps: precursor A pulsing (Step 1), inert gas purge (Step 2), precursor B pulsing (Step 3), and another purge (Step 4), shown in Fig. 1b. In Step 1, the precursor A (commonly metalorganics) is pulsed into the reaction chamber and the molecules are chemically or physically adsorbed on the substrates. In Step 2, an inert gas (e.g. N_2 or Ar) is used to clean the chamber and bring excessive precursor A and by-products out, thus a pure monolayer of adsorbed precursor A is left behind. In Step 3, precursor B (co-reactants) is transported into the chamber by inert gas, and then reacts with the adsorbed precursor A to form a layer of target product. Finally, another purge step is conducted in Step 4 to clean the chamber for the next deposition cycle. For high-aspect-ratio substrates, an "exposure" step (to seal the precursor molecules in the chamber for a prolonged duration) can be added between the pulse and purge steps, which allows the precursors to diffuse into the small pores deep inside the substrates with enough time. All these operations including pulsing, purging, and exposing involved in ALD are automatically controlled by high-speed valves with the preciseness of in the time scale of milliseconds (Fig. 1c). With the appropriate precursor selection and right sequential procedure, the self-limiting nature of ALD reactions is ensured and the composition and thickness of deposition layers can be tuned precisely. Moreover, multiple component films can be deposited by taking three or more precursors into the deposition processes, which might further extend the applications of ALD.

Due to the high reactivity of precursors, ALD can be applied on almost any substrate surface, and this substrate-independent property makes ALD a platform technology, which is particularly suitable to deposit membranes prepared from various materials. However, the deposition mechanism of ALD on "active" (with extensive functional groups, e.g. $–NH_3$ and –OH) and "inert" (with almost no functional groups) membranes is different. For "active" membranes, ALD precursors react with the abundant functional groups quickly, therefore, uniform and conformal deposition layers are formed on the membrane surface and pore walls. For "inert" membranes, although there are barely no reactive sites on the surface, the precursor molecules infiltrate into the subsurface region or material defects to nucleate. With more ALD cycles, the nuclei exceed the subsurface region and then form continuous layers on the membranes [26]. Combining the high reactivity of precursors with low reaction temperature [27–30], ALD can be conducted on temperature-sensitive membranes, which further ensures the applicability of ALD in treating membranes, especially for those less thermotolerant polymeric membranes.

The earliest research work of ALD on separation membranes can be dated back to 1995. Kim and Gavalas used $SiCl_4$ and H_2O as precursors to deposit SiO_2 on the porous Vycor glass for gas separation, and obtained a selectivity of H_2 towards N_2 exceeding 2000 at the expense of a modest reduction in H_2 permeance [31]. In 2006, Triani et al. deposited TiO_2 on track-etched polycarbonate (PC) membranes, which was the first representation utilizing ALD on polymeric membranes. This work showed that the gas conductance of track-etched PC membranes could be controlled by using ALD to adjust pore sizes [32]. In 2011, our group reported the ALD modification of track-etched PC membranes for separation usages in water, and demonstrated the strong capability of ALD in precisely tuning separation properties and improving wettability and chemical stability of membranes. To the best of our knowledge, this is the first time that ALD was employed to modify liquid-separation membranes [33,34].

One of the most attractive advantages for ALD in membrane

modification is that the pore size of membranes can be tailored at the angstrom level. This feature endows ALD with the ability to upgrade the separation precision of membranes, e.g. upgrading the microfiltration membranes to ultrafiltration membranes. Both inorganic and polymeric membranes can be upgraded by ALD modification [35–37]. McCool et al. [35] demonstrated that the pore sizes of silica membranes were reduced by ALD from mesoporous membranes (~3.6 nm) to microporous membranes (~1 nm). Liang et al. [38] confirmed that ALD could precisely tune the pore size of cross-linked lyotropic liquid crystal (LLC) membranes from 0.75 nm to 0.55 nm by only 10 cycles of deposition. Meanwhile, ALD can confer stability, customized wettability, fouling resistance, antimicrobial activity and other properties to membranes. The synergy of these improvements may bring exciting consequences into separation processes. For example, breaking the trade-off effect in membranes is hardly achieved by other modification methods. In contrast, ALD can realize the simultaneous promotion of selectivity and permeability for both polymeric membranes and inorganic membranes through the combination of pore size reduction and enhanced wettability. These results further confirm the great potential of ALD in membrane modification and functionalization.

As a burgeoning field, increasing research works have appeared and deepened our understandings on ALD-enabled membrane modification, functionalization, and preparation. Not just a powerful tool to improve the performance of membranes, ALD also provides a chance to reveal the mechanism of how the physical and chemical properties of membrane surfaces or pores influence the separation. It should be credited that there are a few reviews of ALD on membranes have been published [34,39,40], but most of them are focused on ALD of inorganic materials to improve membrane performances. Little attention has been paid to ALD of polymers on substrate membranes although polymer-deposited membranes exhibited excellent performances. Moreover, some milestone progresses achieved in the past few years, for example, ALD application to hollow-fiber membranes, are not included. In this Review, we summarize and analyze studies on ALD-enabled modification, functionalization, and preparation of separation membranes for water purification and gas separation. This Review is organized basically according to the material nature of the membranes to be ALD treated: polymeric membranes and inorganic membranes. As the majority of works of ALD on membranes is dealing with ALD of metal oxides on polymeric membranes, ALD on polymeric membranes are split into three sections with different focuses. In addition, ALD of polymers and emerging materials on either polymeric or inorganic membranes is newly realized but highly promising, and it is highlighted as two separated sections. This Review aims to show how ALD improves the performance of existing membranes and to prepare new membranes. We expect that this Review can provide clear insights into the ALD-based processes of membrane modification, functionalization and preparation, and attract more interests to solve the bottlenecks in the large-scale application of ALD in the membrane field, thus pushing forward the industrialization of ALD-upgraded membranes.

2. Effects of ALD to membranes

Benefiting from the self-limiting nature and all-gas-phase reactions, ALD can construct deposition layers on both the outer surface and the inner pore walls of membranes with extraordinary uniformity, conformality and precision. With the continuous progresses in precursor synthesis and process development of ALD, the number of materials which can be prepared by ALD keeps expanding. To date, metals, oxides, metal nitrides, metal sulfides, polymers, metal organic frameworks (MOFs), multicomponent hybrid materials, and many other materials have been successfully synthesized via ALD [41]. In general, the effects of ALD to a membrane can be classified into three main aspects: (1) modification, i.e. changing the properties of the membrane [42–47], (2) functionalization, i.e. providing new functions to the membrane [48–51], (3) preparation, i.e. building new separation layers on substrates [52–56] (Fig. 1a). Specifically, the roles of ALD playing in treating membranes can be summarized as the following ones (Fig. 1a):

- Tuning pore size;
- Regulating wettability;
- Improving fouling resistance;
- Enhancing mechanical robustness;
- Improving chemical stability;
- Enabling (photo)catalytic properties;
- Building transitional layers;
- Synthesizing selective layers.

3. ALD of metal oxides on polymeric membranes for direct modification

As the majority of currently used membranes are polymeric ones, most works on ALD-enabled membrane modification are concentrated on polymeric membranes. For the deposited materials, metal oxides, mainly Al_2O_3, TiO_2, and ZnO, are most extensively ALD-deposited on various polymeric membranes for two reasons. One is that these oxides can be easily deposited at fast rates from affordable precursors, and the other is that they show multiple effects in the modification of polymeric membranes. A number of studies have demonstrated that ALD is a generic and efficient strategy to modify almost every type of polymeric membranes. In the ALD-modified polymeric membranes, enhanced performance and new functions are observed, and even the troublesome trade-off effect can be overcome.

3.1. Breaking the trade-off effect

The most striking merit of ALD for polymeric membrane modification is the ability to break the trade-off effect, which means that the selectivity and permeability of membranes can be simultaneously promoted. Xu et al. [42] deposited Al_2O_3 on PTFE membranes and efficiently hydrophilized the membranes. With increasing ALD cycles, the Al_2O_3 granules appeared on the surface of PTFE membranes and the diameter of the fibrils composed of the membranes was gradually increased. After deposited with certain ALD cycles, the fibrils were totally coated by Al_2O_3 and the effective pore size was significantly reduced (Fig. 2a). After 500 cycles of ALD deposition, the water contact angle of PTFE membranes was decreased from ~130° to <20°. Benefiting from the hydrophilized surface and the narrowed pore size, the pure water flux (PWF) and retention towards 190-nm polystyrene (PS) nanospheres of the modified PTFE membranes were increased by 67.7% and 11.4%, respectively (Fig. 2b). This work clearly demonstrates that ALD is able to efficiently break the long-standing trade-off effect of polymeric membranes. This result was confirmed by other researchers depositing different materials on other membranes. As shown in Fig. 2c–d, after conformally deposited with TiO_2, PVDF membranes exhibited progressively reduced water contact angles, and simultaneously improved selectivity and permeability [43]. Simultaneous increase in water permeance and rejection has also been realized in hollow-fiber membranes subjected to appropriate ALD treatment [44,45], which will be discussed in the following section. Additionally, inorganic membranes may also suffer from the trade-off effect, which can be similarly overcome by ALD with suitable materials [57]. We summarize the reported cases of breaking the trade-off effect of membranes by ALD deposition in Table 1.

The size, size distribution, and chemistry of pores play significant roles in determining the selectivity and permeability of a membrane, and synergetic tuning of these factors may break the trade-off effect. The competing effect of pore size reduction and surface hydrophilization is the main reason for ALD of metal oxides to break the trade-off effect of hydrophobic membranes. With increasing ALD cycles, the membrane pores are gradually narrowed, which will enhance the selectivity on one hand while increase the transport resistance on the other. However, the

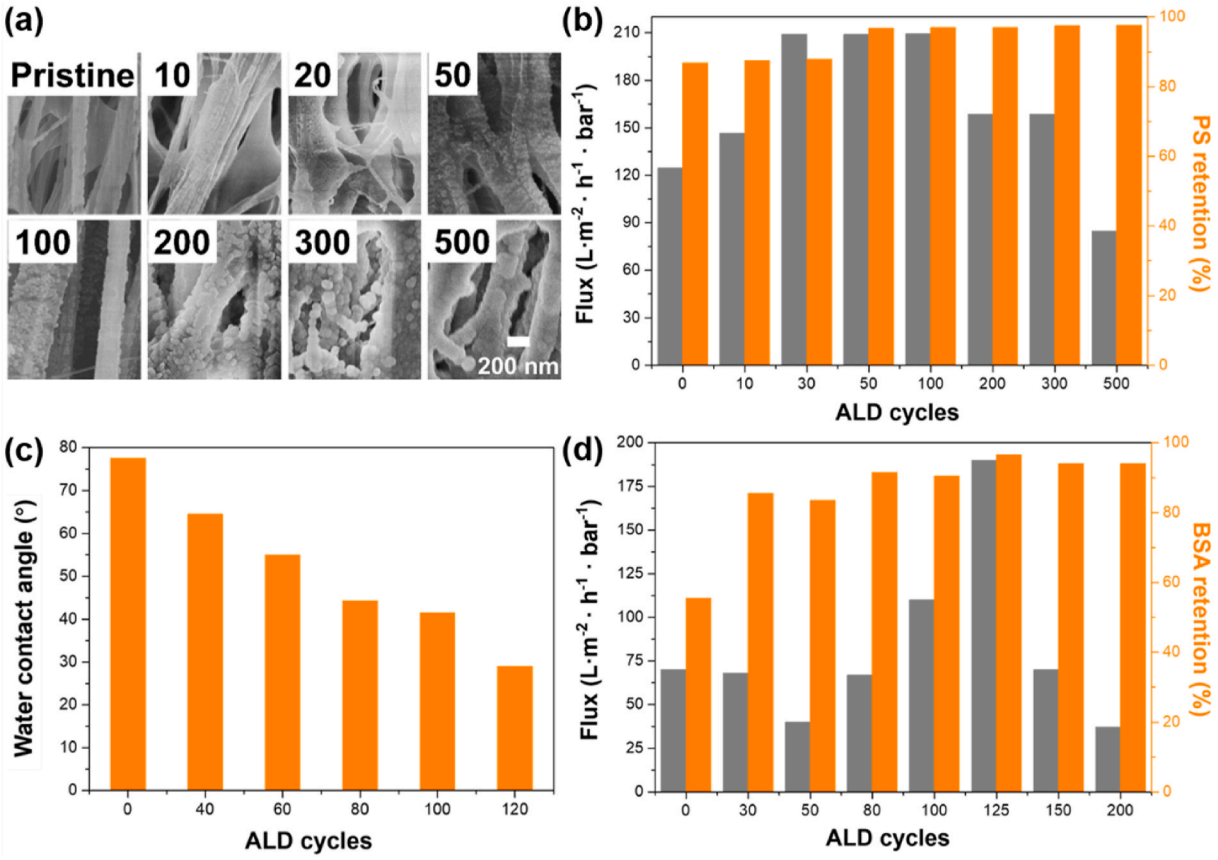

Fig. 2. ALD of metal oxides on polymeric membranes to break the trade-off between permeability and selectivity. (a) SEM images of the pristine and Al_2O_3-deposited PTFE membranes with various ALD cycles; (b) PWF and retention towards 190-nm PS nanospheres of PTFE membranes subjected to Al_2O_3 deposition with various ALD cycles [42]; (c) Water contact angles; (d) PWF and retention towards bovine serum albumin (BSA) of PVDF membranes subjected to TiO_2 deposition with various ALD cycles [43].

Table 1
Reported cases of breaking the trade-off effect of membranes by ALD deposition.

Membrane material	Separation process	Deposited material	ALD cycles	Increment		Ref.
				Permeance	Rejection	
PTFE	MF	Al_2O_3	100	67.7%	11.4%	[42]
PVDF	UF	TiO_2	120	171.4%	72.7%	[43]
PP hollow fibers	UF	Al_2O_3	50	17%	~100%	[44]
PTFE hollow fiber	UF	Al_2O_3	100	96%	21.1%	[45]
Graphene oxide	NF	Al_2O_3	9	107%	36.6%	[57]
PP, plasma-activated	UF	TiO_2	200	22%	213%	[58]
PTFE, plasma-activated	MF	TiO_2	150	154%	~100%	[59]
PP, Nitric acid-activated	UF	Al_2O_3, TiO_2	100	~100%	–	[60]
PVDF, NO_2-activated	UF	ZnO	100	~230%	32.9%	[61]

permeability is regulated by the competition between pore size and surface wettability. Compared to other strategies to improve the hydrophilicity of membranes, ALD renders strong hydrophilicity to membrane pores at a slight expense of reduction in pore sizes because the ALD-deposited layers are conformally coated along the pore walls with a very thin thickness. Therefore, the strong enhancement in hydrophilicity significantly facilitates water transport while the small reduction in pore sizes leads to a slight decrease in water permeance and a more obvious increase in rejection. Consequently, the membranes subjected to suitable ALD of metal oxides exhibit simultaneously improved permeability and rejection. Generally, metal oxides have higher surface energy and better hydrophilicity than polymers. After coated by metal oxides, the hydrophobic polymeric membranes are hydrophilized. Within proper ALD cycles, the positive impact from the hydrophilization is stronger than the negative impact from the pore shrinkage, so the permeability and selectivity are enhanced simultaneously. It should be noted that breaking of the trade-off effect is more evident for membranes prepared from inert polymers such as PTFE and PP [42–45,57] because they will have a profound transition from strong hydrophobicity to hydrophilicity after ALD of metal oxides.

3.2. Boosting separation performance

Although we wish that both selectivity and permeability can be promoted by ALD, it is still worthwhile to slightly sacrifice permeability to obtain a great promotion in selectivity or other desired properties, or

vice versa. Thus, the fouling resistance, mechanical robustness, chemical stability and other properties can be enhanced along with the modification. Metal oxides have been generally used to enhance the hydrophilicity and chemical stability of polymeric membranes. Li et al. [33] deposited uniform and conformal Al_2O_3 layers on track-etched PC membranes. With increasing ALD cycles, the hydrophilicity of track-etched PC membranes was enhanced and the pore size was gradually narrowed with the rate of 0.8 Å per cycle (Fig. 3a), thus the protein retention was enhanced. Moreover, the deposited PC membranes survived from the 5% HCl solution and 1% chloroform ethanolic solution, implying a strongly improved chemical stability. Alam et al. [62] deposited TiO_2 on polyethersulfone (PES) membranes to improve their desalination performance. The NaCl rejection of PES membranes was increased from ~20% to more than 90% at the expense of only ~22% decline in flux. After deposition, the "ridge-and-valley" structure on the membrane surface was coated with TiO_2 layers and the roughness was reduced. The mechanical properties, surface hydrophilicity and fouling resistance of the PES membranes were also enhanced after deposition.

Due to the hydrophobic nature of polymer materials, polymeric membranes are easily fouled by pollutants in separation, which will increase operation costs and decrease the service life of membranes. Therefore, modifications are usually required to improve the fouling resistance of membranes. Typically, the fouling resistance can be enhanced along with the improvement of hydrophilicity. Metal oxides including TiO_2, Al_2O_3 and ZnO were usually used to enhance the fouling resistance of polymeric membranes [46]. Benefiting from the self-limiting property of ALD, metal oxides coated on the pore wall uniformly, ignoring the complex structure of membranes (Fig. 3b). Owing to the smoother surface and better hydrophilicity, the ZnO-deposited PVDF membrane exhibited an excellent fouling resistance, and its static adsorption towards protein and polysaccharide was decreased by 43.2% and 73.0%, respectively. Thermodynamic investigation further confirmed that the ZnO deposition layer had the lowest spontaneous possibility to adsorb contaminants. To clearly illustrate the mechanism, the extended Derjaguin-Landau-Verwey-Overbeek theory was employed to analyze the fouling resistance improvement observed on ZnO deposited PVDF membranes [63]. It was revealed that the repulsive energy between the target contaminant (sodium alginate, SA)

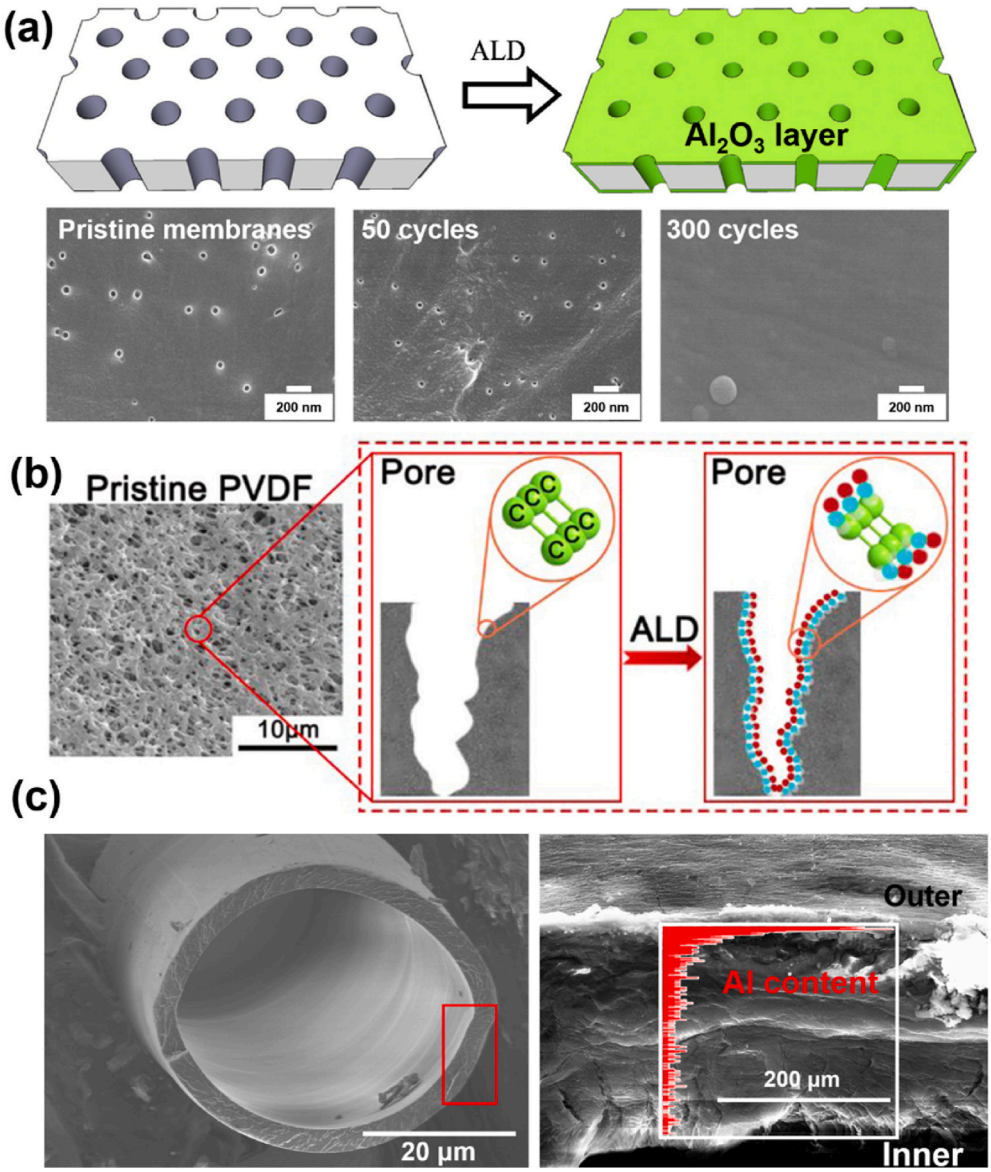

Fig. 3. ALD of metal oxides to enhance the performance of polymeric membranes. (a) The diagram and SEM images of uniform Al_2O_3 layers deposited on the track-etched PC membranes [33]; (b) Conformal metal oxides layers deposited on the porous PVDF membranes [46]; (c) The morphology and Al_2O_3 distribution cross the fiber wall of PP hollow-fibers membranes subjected to ALD of Al_2O_3 for 200 cycles [44].

and the membrane was raised after ZnO deposition, while the attractive energy between them was weakened. Therefore, the anti-fouling ability of the membrane was enhanced. Moreover, uniform ZnO layers decreased the attachment of SA molecules, which further improved the fouling resistance. That is, after deposition with hydrophilic metal oxides, the interaction between membrane surface and contaminants is weakened, and the uniform deposition layer will greatly reduce the physical adhesion of contaminants. Consequently, the fouling resistance of polymeric membranes is efficiently improved by ALD of metal oxides.

In addition to the flat-sheet polymeric membranes, ALD can also be used to modify hollow-fiber membranes and improve their separation performance. Jia et al. [44] used ALD to modify porous PP hollow-fiber (PPHF) membranes. With 200 cycles of Al_2O_3 deposition, the Al element could be detected throughout the hollow fibers including the inner walls, implying that ALD was also applicable to the modification of hollow-fiber membranes although they possess a less accessible configuration. However, the Al element density was decreased gradually inward the tube wall (Fig. 3c). This was ascribed to the reduced diffusion of precursors through the membranes as the pores in the hollow-fiber membranes kept shrinking with rising ALD cycles. After deposited with certain cycles of Al_2O_3, the water flux and rejection towards BSA of the PPHF membranes were both increased. Importantly, ALD enhances the mechanical strength of the PPHF membranes. The elongation at break of the membranes was increased by more than 6 times after deposition. Due to the high reactivity and subsurface nucleation mechanism, the precursor, trimethylaluminium (TMA), might react with the polymer chains and form C–Al–C bonds, thus the mechanical strength of the membranes was enhanced [64]. In the ALD of membranes, many parameters (e.g. precursor dosage, purge time, reaction temperature, and reaction pressure) influence the deposited effect as well as the performance of the deposited membranes. Therefore, optimization of the deposition parameters might be tedious and labor-consuming. To solve this problem, Xiong et al. [45] used computational fluid dynamics (CFD) to screen the deposition parameters in the modification of hollow-fiber PP membranes. Simulation results showed that the reaction pressure (related to precursor dosage), fluid flow (related to precursor distribution), and substrates reactivity had significant influences on ALD deposition. Under CFD-optimized deposition parameters, the pure water flux and rejection towards 22-nm SiO_2 microspheres of the hollow-fiber membranes were increased by 96% and 21% after deposition, respectively. Moreover, the deposited membranes exhibited an obvious decrement in static adsorption of BSA.

3.3. Enabling new functions

By choosing appropriate ALD precursors and deposition processes, various materials and structures can be directly deposited on polymeric membranes to achieve new functions beyond membrane separation. The

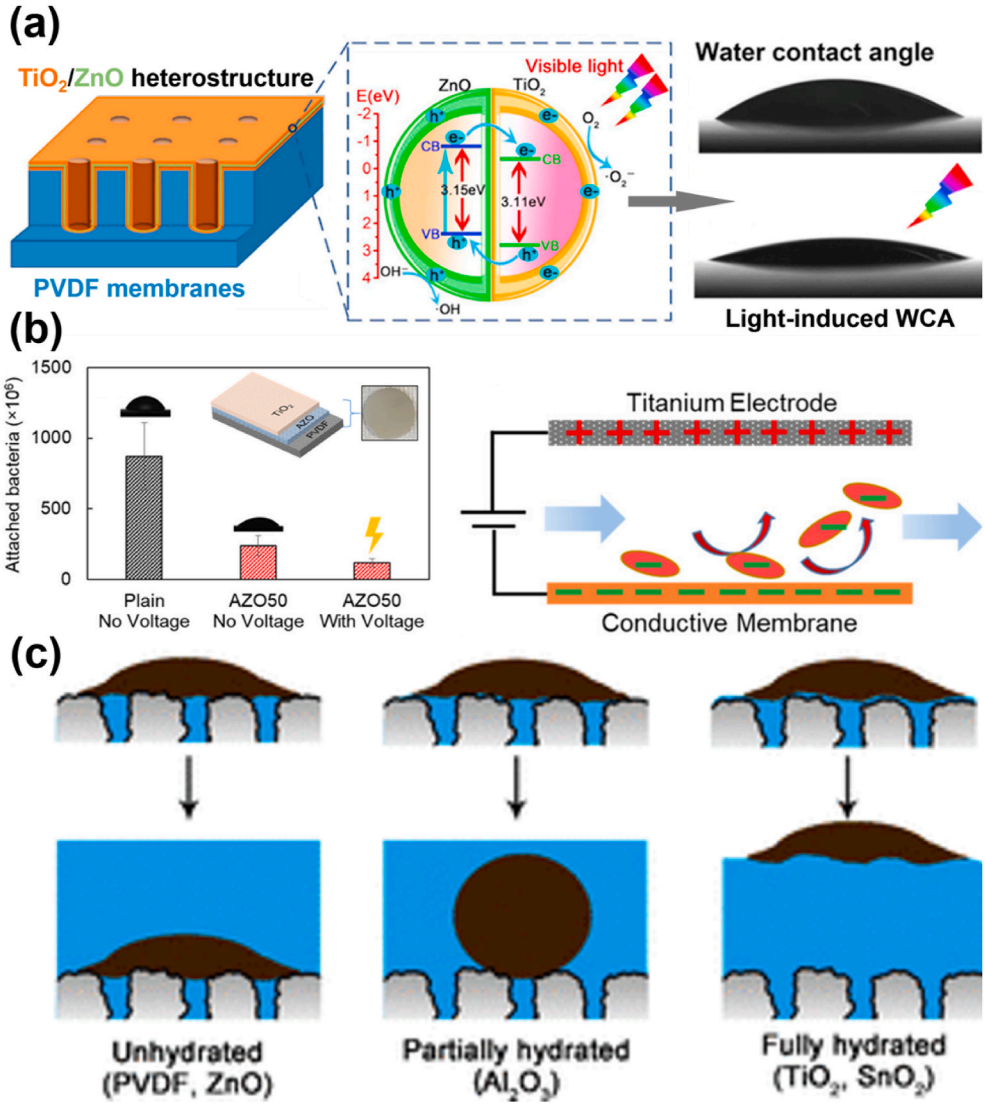

Fig. 4. ALD of metal oxides to endow new functions to polymeric membranes. (a) The structure and light-induced hydrophilicity of ALD-modified PVDF membranes and the photocatalysis mechanism of TiO_2/ZnO type II heterostructures [48]; (b) The bacteria attachment of AZO50 membranes under −1 V and the application diagram of conductive membranes [49]; (c) Speculated mechanisms of oil on the surfaces of pristine PVDF membranes and membranes ALD-coated with different metal oxides [51].

photocatalytic property can be directly obtained for membranes deposited with semiconducting oxides such as TiO_2 and ZnO. Li et al. [48] utilized ALD to deposit 3D TiO_2/ZnO type II heterostructure on PVDF membranes, which endowed the membranes with light-induced hydrophilicity and photocatalytic ability (Fig. 4a). With the optimum ALD sequence (1 cycle of TiO_2 and 3 cycles of ZnO), the water contact angle (WCA) was decreased by 82.6% and the flux was increased by 33.5% after light irradiation. The TiO_2/ZnO type II heterostructures on PVDF membranes removed ~80% methylene blue under visible light irradiation. Moreover, the fouling resistance of the deposited membranes was also improved. The morphology of ALD-deposited metal oxides is influenced by many factors such as interactions between precursors and substrates, deposition temperature, precursor dosage, and deposition mode. By controlling the precursor dosage and deposition mode, ZnO was deposited on the electrospun nylon nanofibrous membranes with different morphologies, i.e. ZnO nanoparticles (NPs), highly dense ZnO NPs, and 27-nm thick ZnO layer, which endowed the membranes with varied photocatalytic activities [65]. All the ZnO-deposited membranes could degrade rhodamine B (RhB) under UV irradiation, and the membranes coated with highly dense ZnO NPs showed the best performance because of the higher surface roughness and surface area. Except for the photocatalytic function, ALD can also introduce electrochemical activity to membranes. Yang et al. [49] used ALD to deposit conductive aluminum-doped zinc oxide (AZO) layers onto PVDF membranes to enhance the fouling resistance (Fig. 4b). One layer of AZO was prepared by 20 cycles of ZnO deposition and subsequent 1 cycle of Al_2O_3 deposition. To avoid corrosion in water, a thin layer of TiO_2 (~11 nm) was ALD-coated on the AZO surface as the protective layer (inset in Fig. 4b), which endowed the AZO films with excellent stability and exhibited no corrosion in water for 7 days. The thicker AZO films showed better electrochemical performance but worse permeability. The bacterial attachment on the membrane with 50 AZO layers was 72% lower than the pristine PVDF membrane. After applying a 1.5 V voltage onto the AZO50 membranes, the bacterial attachment was further decreased to 86%. Other functions such as adsorption can also be obtained depending on the nature of the deposited materials. Xiong et al. [50] deposited ZnO on PTFE membranes and bestowed the membranes on the ability of dye adsorption. Adsorption tests showed that the deposited PTFE membranes removed both positively charged RhB and negatively charged Acid Orange 7 molecules from water with satisfying efficiency. The deposited PTFE membranes showed no obvious performance degradation after reused for several times. The functions enabled by ALD to membranes are summarized in Table 2.

ALD of metal oxides on polymeric membranes may significantly change the wettability of polymeric membranes. Interestingly, the change in wettability can be in the opposite way. In most cases, deposited oxides convert originally hydrophobic surfaces to be strongly hydrophilic, thus enabling an oil/water separation function to the membrane by preferentially allowing water to pass. Oil-containing wastewaters are hard to be treated by conventional polymeric membranes. This is because the membranes are easily fouled by viscous and hydrophobic oils, which will lead to severe flux reduction and lifetime decay. By depositing Al_2O_3, ZnO, TiO_2, or SnO_2 layers with a thickness of only ~10 nm on PVDF membranes, Yang et al. [51] endowed PVDF membranes with strong oleophobicity. Experiments and molecular dynamic simulation showed that the TiO_2- and SnO_2-deposited membranes had tightly bound hydration layers on the surface, thus a water cushion formed on the membranes to cut the interaction between oil and membrane surface. The totally hydrated membranes utilized the immiscibility between water and oil to acquire excellent crude-oil-repellent property (Fig. 4c). Further, even superhydrophilicity can be obtained by ALD of metal oxides on polymeric substrates with particularly roughed surfaces. Li et al. [66] deposited TiO_2 layers onto PP nonwovens, which endowed the originally hydrophobic PP nonwovens with superhydrophilicity and underwater superoleophobicity. Due to the customized wettability, the deposited PP nonwovens showed a self-cleaning capacity which removed the attached organic solvents only by water washing. The deposited PP nonwovens also inherited the chemical stability from TiO_2 and could be used in harsh solutions. Counterintuitively, ALD of metal oxides may also turn hydrophilic membranes to be hydrophobic. By depositing few cycles of Al_2O_3 or TiO_2 onto cellulose-based nanopaper membranes, the C–C/C–H bonds on the membrane surface were increased, thus turning the initially hydrophilic membranes to hydrophobic [68]. The increasing C–C/C–H bonds came from the unreacted methyl groups of organometallic precursors, or adsorbed adventitious carbon on the membrane surface after deposition. The deposited membranes withstood harsh sonicating treatments both in nonpolar organic solvents and in water. Density functional theory calculation exhibited that the strength of the hydrogen bond between celluloses was enhanced by the M–OH terminations on metal oxides, thus decreasing the hydration effect between fibrils and solvents and consequently enhancing the robustness of cellulose membranes. The modified membranes showed strong resistance towards water and strong affinity towards oil like *n*-hexane, which suggested their potential applications in oil/water separation.

Interestingly, metal oxides deposited on polymeric substrates may show variable wettability depending on the amount of the deposited oxides, that is, the ALD cycle numbers. After deposition of Al_2O_3, the thermal and mechanical properties of poly(vinyl alcohol-co-ethylene) (EVOH) nanofibrous aerogels (NFAs) were strengthened [67]. The Al_2O_3 deposition layer on the surface or inner parts of the aerogels showed no difference after 100 cycles of deposition. This result confirmed that ALD could deposit uniform films onto the highly porous substrates. It was worth noting that the aerogels exhibited hydrophobicity with lower ALD cycles (<8 cycles) and hydrophilicity with higher ALD cycles (>8 cycles). There were structural and chemical reasons for this wettability transition. With less ALD cycles (<7 cycles), the Al_2O_3 preferred to be deposited as small bulges on the fibrils. Combining the rough fibrils and highly porous NFAs, hierarchical structures were constructed to store more air and enhanced the hydrophobicity of the EVOH NFAs. With more ALD cycles, the C–OH bonds on NFAs were gradually turned into hydrophilic Al_2O_3, and the hierarchical structures were slowly destroyed by the forming of uniform Al_2O_3 deposition layers, thus the WCAs decreased with more ALD cycles. The aerogels underwent 6 cycles of ALD exhibited the strongest hydrophobicity, while the aerogels with 8 cycles of ALD began wettability transforming. Meanwhile, the 6-cycle-deposited aerogels had high deformability and excellent elastic resilience, which maintained 70% of the initial maximum stress and Young's modulus after 500 cycles of stress-strain tests. Considering the excellent mechanical stability and strong hydrophobicity, the 6-cycle-deposited aerogels were high-performance oil absorbents, which exhibited uptake capacities from 31 to 73 g g^{-1} towards different organic solvents with superior reusability. We note that this work it is not directly dealing with membranes. However, the strategy to tune the wettability by ALD cycles can be readily extended to prepare functional membranes with switchable wettability.

Table 2
New functions of membranes enabled by ALD.

Membranes	Deposited materials	Function	Ref.
PVDF	TiO_2/ZnO	Fouling resistance; Photocatalysis	[48]
Nylon nanofibers	ZnO	Photocatalysis	[65]
PVDF	Al_2O_3-doped ZnO/TiO_2	Fouling resistance; Conductivity	[49]
PTFE	ZnO	Adsorption	[50]
PVDF	Al_2O_3, ZnO, TiO_2, SnO_2	Oil repellency	[51]
PP nonwovens	TiO_2	Oil repellency	[66]
EVOH nanofibrous aerogels	Al_2O_3	Oil absorption	[67]

3.4. Upgrading NF and RO membranes

It is interesting to note that most works on the ALD modification/functionalization of membranes have been concentrated on microfiltration (MF) and ultrafiltration (UF) membranes, while much less attention is paid to nanofiltration (NF) and reverse osmosis (RO) membranes. Nikkola et al. [69] reported the first work on ALD modification of RO membranes. They found that the membrane deposited at a lower temperature (70°C) exhibited a more hydrophilic surface, which endowed the RO membrane with better fouling resistance and higher permeability. Although the NaCl rejection was decreased from 95.5% to 89.7% after 10 cycles of Al_2O_3 deposition at 70°C, the salt solution flux was increased from 5.50 to 15.05 $L{\cdot}m^{-2}{\cdot}h^{-1}$. Zhou et al. [70] made a systematic investigation on the effect of ALD deposition of TiO_2 on the performance of commercial polyamide NF and RO membranes. They used tetrakis(dimethylamido) titanium-(IV) (TDMAT) as the precursor. As shown in Fig. 5a, due to the size differences (NF membrane pore > TDMAT > RO membrane pore), the TDMAT molecules had access to the NF membrane pores, while were restricted to the RO membrane surface. Therefore, the pore reduction effect by ALD in NF membranes was more obvious than in RO membranes. NF membranes showed reduced pore size and increased rejection towards NaCl and $CaCl_2$ after merely 5 cycles of deposition. This is in stark contrast in the ALD modification of MF and UF membranes, which typically requires several hundreds of ALD cycles to evidently reduce the pore sizes and thus to tighten the rejection. For RO membranes, both the permeability (increased by less than 3%) and NaCl rejection (decreased from 99.8% to 99.5%) were changed very little within 5 cycles of deposition. However, the surface charging property of RO membranes was changed and the fouling resistance was enhanced. Another work also showed that ALD of metal oxides on NF membranes enhanced the reversible fouling resistance and water flux without sacrifice of ion removal efficiencies [71].

In addition to directly deposit metal oxides on existing RO membranes, ALD can also be involved in the formation of thin-film composite (TFC) RO membranes to improve the separation performance. Zarshenas et al. [72] utilized ALD to deposit uniform TiO_2 layers onto PES substrate membranes as an intermediate layer between the PA selective layer and the substrate. Owing to the precise thickness control and the subsurface growth mechanism of metal oxides on polymeric substrates during ALD, the nanoscale TiO_2 layers firmly adhered to the PES substrates. After TiO_2 deposition, the hydrophilicity, chemical and physical stabilities of PES membranes were enhanced. Meanwhile, the affinity between amine monomer and PES membranes was also improved by the TiO_2 layers. As a consequence, after 100 cycles of TiO_2 deposition and interfacial polymerization of PA, TFC membranes with thinner and smoother PA active layers were obtained (Fig. 5b). Compared to the counterpart without the TiO_2 intermediate layer, the permeance and salt rejection of thus-prepared membrane were increased by ~29% and ~4%, respectively. As demonstrated by these results, ALD is particularly suitable and highly efficient for the modification of NF and RO membranes because of its atomic level precision in tuning the thickness of the depositing layers. Owing to the extremely small pore size (<2 nm) of NF membranes and the compact PA layer of RO membranes, only few cycles of ALD are enough to complete the modification and enhance the performance of membranes. However, due to the dimension difference between ALD precursors and NF/RO membrane pore size, the deposition layers can be deposited on surfaces and into pores of the NF membranes, while only on surfaces of the RO membranes. Therefore, the improvements of NF membranes are in the similar mechanism with the MF/UF membranes, while the improvements of RO membranes are originated from the

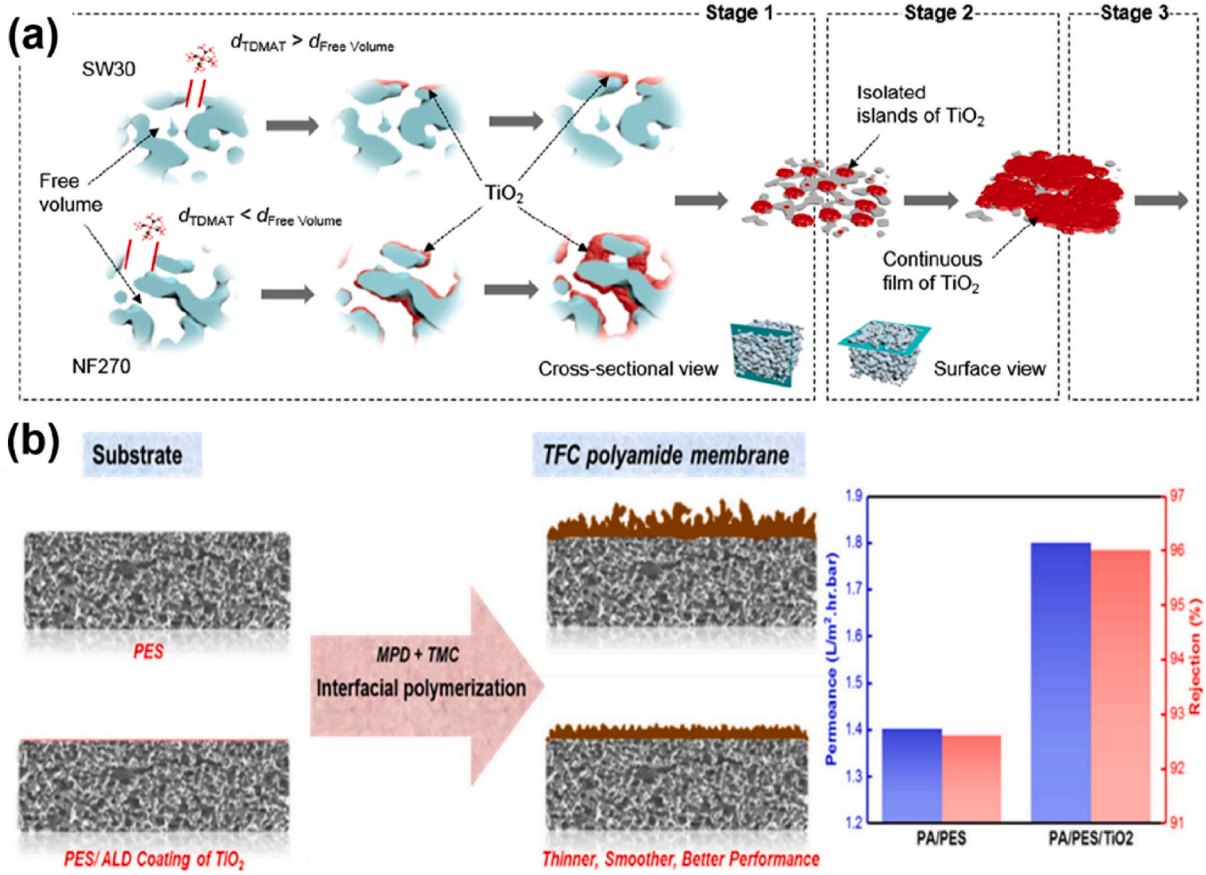

Fig. 5. ALD of metal oxides to improve the performance of NF and RO membranes. (a) Schematic illustration of TiO_2 ALD on RO and NF membranes [70]; (b) Uniform TiO_2 layers deposited on the PES membranes as intermediate layers and improved performance of the TFC RO membranes [72].

change of surface properties. It should be noted that the highly hydrated structures of NF and RO membranes might not withstand the high deposition temperature or vacuum environment during the ALD process, which will cause severe structure destruction and irretrievable performance degradation. Therefore, careful selection of deposition parameters or pretreatment to stabilize the vulnerable PA layers is necessary to ensure the performance of the deposited NF and RO membranes. Moreover, using ALD to modify the surface and structure of substrates of NF/RO membranes and thus to influence the interfacial polymerization process may be an indirect but effective way to improve the performance of these membranes.

4. ALD on surface-activated polymeric membranes

Although ALD can be conducted on almost any polymeric substrates, activated membrane surfaces can provide more reactive sites and require low ALD cycles to form conformal and continuous films than inert membranes. Therefore, pretreatments to activate membrane surfaces will greatly lower the threshold for ALD to break the trade-off effect. Among all activation methods, plasma and acid oxidation treatments are commonly used to pretreat polymeric membranes before ALD. To explore the difference between PP membranes with and without plasma activation, Xu et al. conducted TiO_2 deposition on pristine and plasma-activated PP membranes [58]. Different from the pristine membrane, there was no nucleation stage during ALD on the plasma-activated membrane. The TiO_2 layers exhibited smoother surfaces at the very initial stage. Due to the rapid growth rate and smooth surface, the activated membranes exhibited obvious hydrophilization effects (Fig. 6a). The rejection of the membranes towards 22-nm SiO_2 nanospheres was increased from ~30% to ~100%, and the flux exhibited a 22% increment after 200 cycles of deposition, showing the efficiency of surface activation and confirming again the ability of ALD

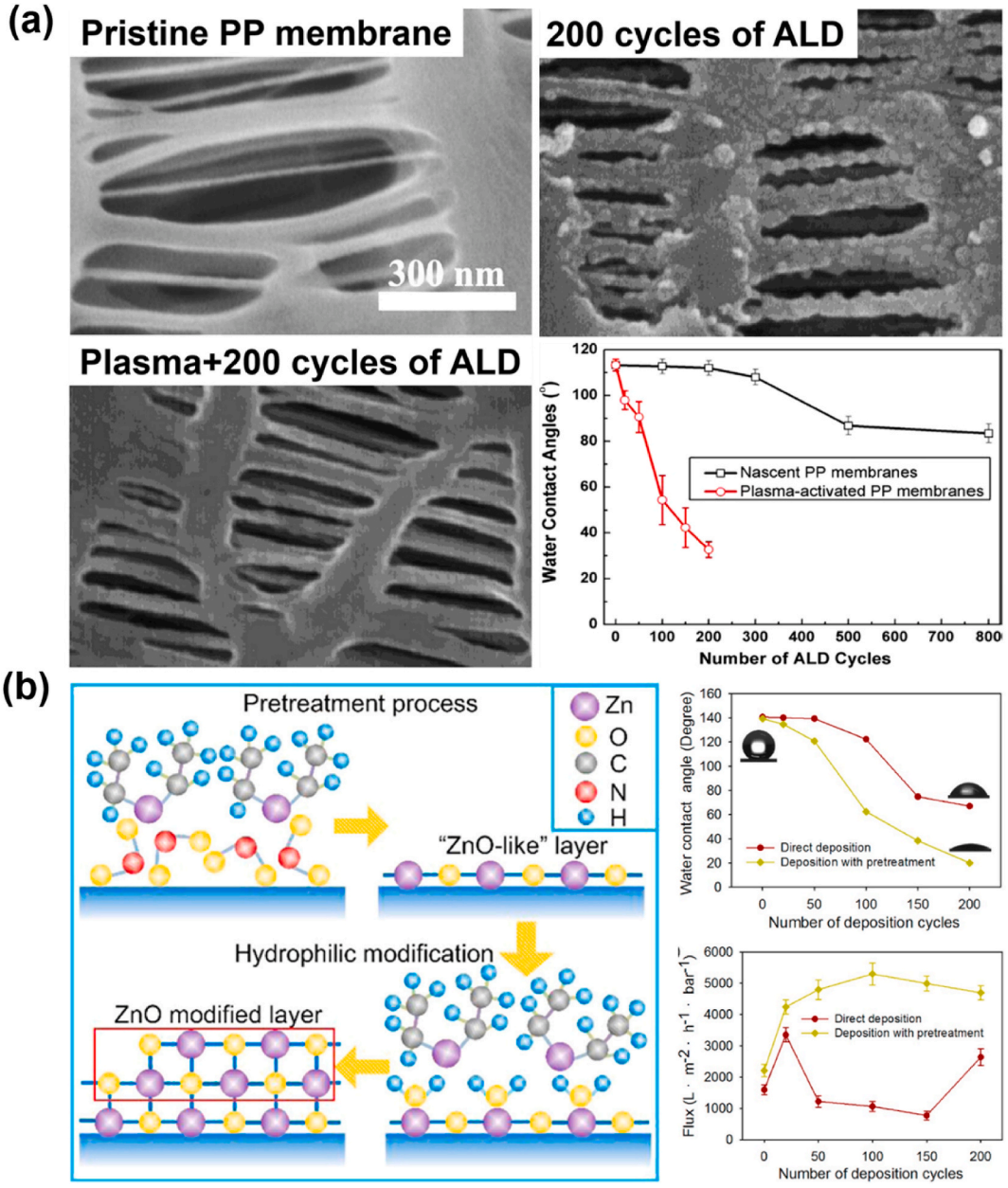

Fig. 6. ALD on surface-activated polymeric membranes. (a) SEM images of pristine and 200-cycle-deposited PP membrane with and without plasma activation, and the WCA changes of the deposited PP membranes with and without activation [58]; (b) The mechanism diagram of NO_2 activation and ALD modification of PVDF membranes, and the hydrophilicity and flux of the deposited PVDF membranes with and without pretreatment [61].

to break the trade-off between permeability and selectivity. The significant role of surface activation by plasma in facilitating the ALD process on PP membranes was confirmed in another work. Chen et al. [73] demonstrated that the plasma-activated PP membranes (used as separators of lithium-ion batteries) required only 20 cycles of ALD to achieve conformal deposition of TiO_2 while the pristine PP membrane required 500 cycles. Except for PP membranes, PTFE membranes with extremely inert surface could also be easily modified by the same "plasma activation + TiO_2 ALD" strategy [59]. In order to simplify the activation process, Chen et al. [60] utilized nitric acid oxidation to activate the PP membranes instead of plasma activation. The nitric acid oxidation generated oxygen- or nitrogen-containing functional groups on the PP membranes, which provided rich sites for the rapid surface growth of metal oxides in the ALD mode. The flux of the modified membranes was doubled after Al_2O_3 or TiO_2 deposition and their rejection remained unchanged. Note that the Al_2O_3-deposited membranes exhibited higher flux increment than the TiO_2-deposited ones because of the faster growth rate of Al_2O_3 and the stronger hydrophilicity of the Al_2O_3-deposited surface. NO_2 has also been used to activate polymeric membranes. To improve the compatibility between the activation layer and the deposition layer, Li et al. [61] used NO_2 to activate PVDF membranes and then reacted with diethyl zinc (DEZ) to form ultrathin "ZnO-like" layers as the activation layer. Comparing with directly depositing ZnO on PVDF membranes, their activated membranes showed higher permeability, better hydrophilicity, larger reduction in pore size, and smoother surface (Fig. 6b). The flux and BSA rejection of the original PVDF membrane were 1594 $L{\cdot}m^{-2}{\cdot}h^{-1}{\cdot}bar^{-1}$ and 73%, respectively. After activation and 100 cycles of ALD deposition, the membrane exhibited a remarkably high flux of 5261 $L{\cdot}m^{-2}{\cdot}h^{-1}{\cdot}bar^{-1}$ and a BSA rejection of 97%. In contrast, the flux and BSA rejection of the directly deposited membrane were lower than 2000 $L{\cdot}m^{-2}{\cdot}h^{-1}{\cdot}bar^{-1}$ and 85%, respectively.

Polyphenol coating is a more generic strategy to provide active groups to membrane substrates. Polyphenol can strongly bind with almost every type of polymeric membranes and the active groups will provide considerable reactive sites for the following ALD processes. DeStefano et al. [74] coated a layer of polydopamine (PDA) on PVDF membranes and subsequently deposited TiO_2 on the PDA-coated membranes. The nonlinear modification result was quite different from the plasma- or oxidation-activated membranes. The WCAs of membranes reached 69° after 60 cycles of TiO_2 deposition, while the WCA was sharply decreased to ~20° after 75 cycles of deposition, and was then increased to 40–50° after 90 cycles of deposition. This is because the surface property of ALD-modified membranes is determined by the interplay of the chemistry, structure of the deposited materials, as well as the surface chemistry of the substrates. Yang et al. [75] coated polyphenols on hydrophobic PVDF membranes and then conducted TiO_2 ALD on the membranes. Comparing with the membranes only modified by ALD, the PVDF membranes treated with tannic acid sensitization and ALD exhibited outstanding underwater oleophobicity with good mechanical robustness. The modified membranes were used to separate crude oil-in-water solutions with high efficiencies and outstanding reusability. Although surface activation requires additional efforts and sometimes is tedious, it is significant or even indispensable to the low-surface-energy polymeric membranes. As we discussed above, with sufficient reactive sites, the ALD process on polymeric membranes can skip the time-consuming nucleation and grain growth stage, thus forming uniform films rapidly. Consequently, the efforts to perform surface activation are rewarded by the significantly reduced deposition durations as well as the higher quality of the deposition films.

5. ALD on polymeric membranes for indirect functionalization

ALD-deposited materials may exhibit additional activities to allow further modifications, or can be used as substrate materials to construct new functional layers on the membrane matrices. Therefore, utilizing ALD-deposited materials in an indirect way may bridge the gap between the polymeric membranes and new functional layers to prepare high-performance membranes or empower new functions. An interesting example is using ALD-deposited nanoparticles as seeds to grow one-dimensional structures. PTFE membranes have been widely used in gas purification processes because of their high gas permeation and stability (chemical, mechanical, and thermal) [76]. However, this usage of PTFE membranes is facing some challenges. Firstly, the membrane pores may be blocked by small particles carried in the gas during the separation processes, thus sharply decreasing the gas flux. Secondly, the membranes are easily fouled by microorganisms due to the inherent strong hydrophobicity. Thirdly, there are some inevitable molecular contaminants in the polluted gases, which cannot be purified by the separation effect of PTFE membranes. To solve these problems, Zhong et al. [77] deposited ZnO on PTFE membranes as seed layers to hydrothermally grow aligned ZnO nanorods (Fig. 7a). The airborne nanosized and microsized particles were trapped by the ZnO nanorods, while the voids between ZnO nanorods allowed air to flow through the membrane with low resistance. Moreover, the ZnO nanorods with antibacterial activity sterilized 99% Gram-positive and -negative bacteria. To further enhance the antibacterial property of PTFE membranes, Ag nanoparticles were loaded onto the ZnO nanorods and the dynamic antibacterial efficiency of this PTFE membrane was increased to ~100% [78]. Moreover, PTFE membranes functionalized with ZnO nanorods exhibited a 53% degradation efficiency to formaldehyde under UV irradiation, and its efficiency reached 60% after further coated with Ag particles. Similarly, Zhang et al. [79] used ALD to deposit TiO_2 nanoparticles on PTFE UF membranes, then turned TiO_2 nanoparticles into arrays of nanorods by solvothermal synthesis. After 200 cycles of TiO_2 deposition and solvothermal growth, both the antibacterial properties and hydrophilicity of the modified PTFE membranes were enhanced, empowering the PTFE membranes excellent reusability in wastewater treatments (Fig. 7b). The bacteria attachment on thus-functionalized PTFE membrane was significantly reduced to 3.3% of that of the pristine one. Meanwhile, the sharp TiO_2 arrays could puncture the bacteria and cause the death of most bacteria. When exposed to sunlight, TiO_2 arrays coated on PTFE membranes generated hydroxyl radicals and further improved the antibacterial activity of the PTFE membrane.

Kong et al. [80] prepared low-cost oil/water separation membranes by ALD depositing Al_2O_3 on filter papers as functional layers followed by modifying the Al_2O_3 layers with silane coupling agents. Thus-treated filter papers exhibited strong hydrophobicity and oleophilicity, which were used to separate various oil/water mixtures and showed overall removal efficiencies higher than 90%. Xiong et al. [81] deposited ZnO on the polyethylene terephthalate (PET) nonwoven fabrics as seed layers to grow ZnO nanorods. Due to the amphiphilicity and hierarchical structure of the ZnO nanorods, water or oil was stored in the "forest" of ZnO nanorods and formed stable liquid films, thus the modified membranes acquired the ability to separate water and oil (Fig. 7c). Because of the immiscibility between water and oil, the water liquid film on the membrane surface separated water from the mixture and vice versa. This idea was also used on copper meshes to fabricate membranes decorated with densely grown ZnO nanowires [82]. By using gravity as the driven force, the nanostructured mesh membranes exhibited a high separation efficiency (>99.7%) as well as a flux up to 4.0×10^5 $L{\cdot}m^{-2}{\cdot}h^{-1}$. Huang et al. [83] used nanoprinted PTFE membranes as substrates for TiO_2 deposition, and then fluorinated the deposited membranes with fluorine-containing silanes. Benefitting from the rough structure and low surface energy, the functionalized membranes exhibited superior omniphobicity and consequently excellent performance in membrane distillation. The membranes showed a high flux of 34 L m^{-2} h^{-1} and ~100% salt rejection with impressive durability and stability, and ~91% of the initial flux was preserved after 3 cycles of fouling-cleaning tests.

Metal alkoxides as a new form of inorganic-organic hybrid materials which can be deposited by ALD, have also been used intermediates to

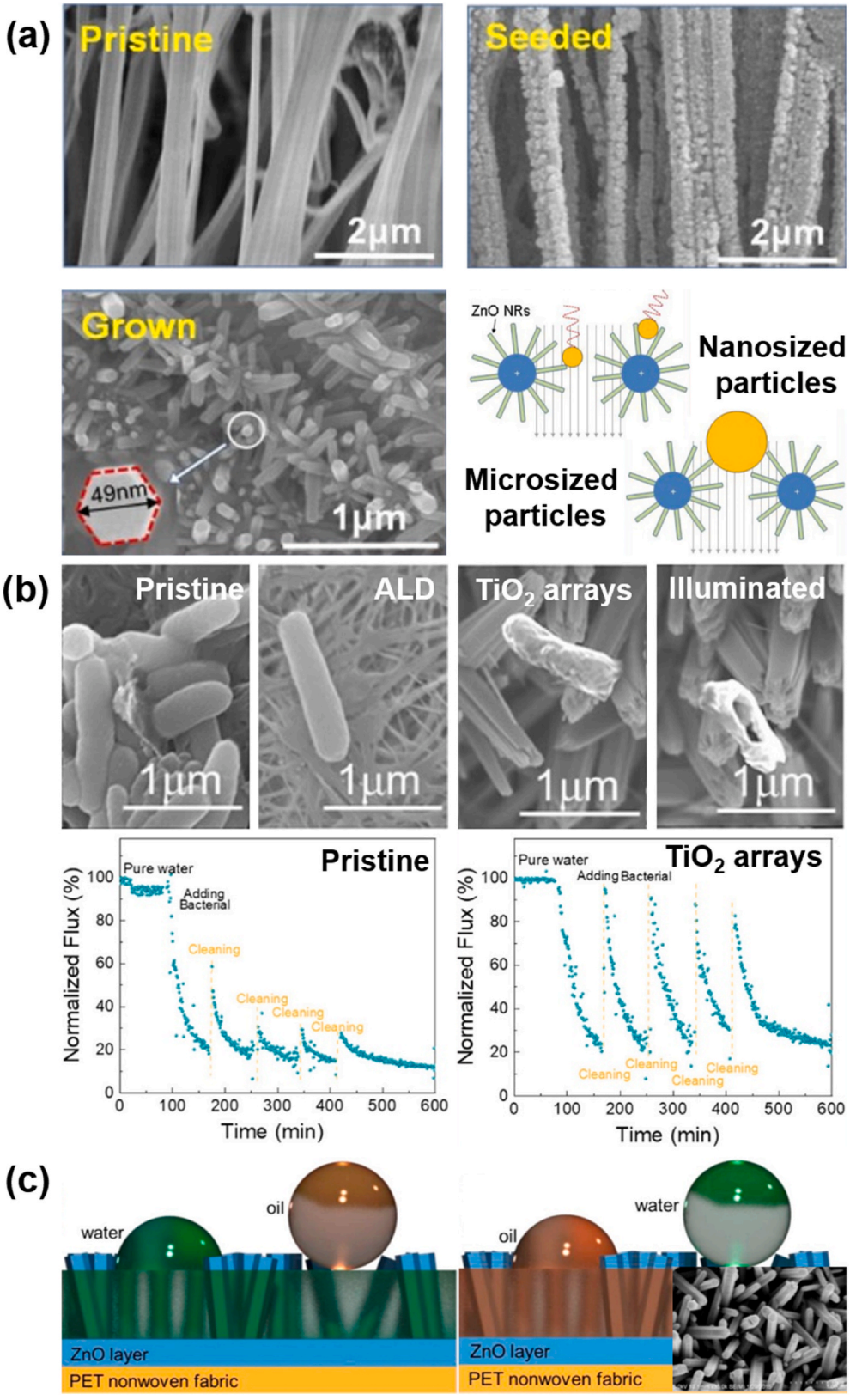

Fig. 7. ALD of transition layers on polymeric membranes to render new functions. (a) The SEM images of the pristine, ALD-seeded, and ZnO-nanorods-grown PTFE membranes and the separation mechanism of the functionalized PTFE membranes [77]; (b) The morphology of bacteria on the surface of PTFE membranes subjected to different treatments and the reusability tests of the pristine and functionalized PTFE membranes [79]; (c) The water and oil films formed on the surface of the PET nonwoven membrane to separate water or oil from water/oil mixture. The inset showed the ZnO nanostructures on the modified membranes [81].

functionalize membranes. By heating or solvent etching, these hybrid materials will lose their organic components, leading to porous structures of metal oxide structures [84,85]. Based on the transition from dense metal alkoxides to microporous metal oxides, new separation layers can be constructed on substrate membranes. Chaudhury et al. [52] used TMA and ethylene glycol (EG, HO-$(CH_2)_2$-OH) as the precursors to deposit alucone (aluminium alkoxide) on the surface of a commercial PA NF membranes. Thanks to the partial organic nature of alucone, the deposited layer presented excellent compatibility with the PA selective layer of the NF membrane. During the initial nucleation

stage, the TMA preferred to react with the functional groups in the PA layer rather than with EG. Then the reaction between TMA and EG was enhanced and gradually became the dominant reaction on the membranes. After deposition, the modified membranes were immersed in water for 3 days to convert the alucone into porous alumina. These processes changed the composition, pore size, and fixed charge of the membrane surface, which affected its dielectric, steric, and electrostatic properties. As a result, thus-modified membrane exhibited different permselectivities towards Na^+ ions and Mg^{2+} ions, and showed better capacity to soften hard waters. The modified membrane softened brackish water (619 mg L^{-1} as $CaCO_3$) to "hard" water (165 mg L^{-1} as $CaCO_3$) while the pristine membrane could only soften the brackish water to "very hard" water (223 mg L^{-1} as $CaCO_3$). The transition of dense metal alkoxides to microporous metal oxides has also been employed to build new separation layers on inorganic membranes, which will be discussed in the following section.

6. ALD on inorganic membranes

Compared to their polymeric counterparts, inorganic membranes are much more tolerant to high temperatures, and usually carry rich hydroxyl groups on the surface, allowing fast ALD deposition conformally along the pore walls. Possibly because of this reason, the first work of ALD application in separation membranes was performed by depositing a thin layer of SiO_2 on porous Vycor glass membranes at the temperature of 700 or 800°C for H_2/N_2 separation, which was reported in the year of 1995 [37].

Similar to the ALD modification to polymeric membranes, ALD was mainly used to finely tune the pore sizes of inorganic membranes and to give new functions to them. The pore size of a commercial ZrO_2 MF ceramic membrane could be tuned from 50 nm down to 0 nm by depositing different cycles of Al_2O_3 (Fig. 8a) [86]. More importantly, the deposition of Al_2O_3 could be restricted only on the surface or penetrated into the pores by regulating the exposure time. With longer exposure times, the pore size reduction was more obvious and the membranes were modified more effectively. After 600 cycles of ALD with 10 s exposure time, the MF membranes were successfully turned into UF membranes. This work also confirmed the versatility of ALD, which showed the ability to fulfill different goals by tuning the deposition parameters. By omitting the exposure time, TiO_2 deposition was restrained exclusively on the near-surface region of UF ceramic membranes and only the pores in the separation layer were narrowed (Fig. 8b) [87]. After only 40 cycles of deposition, the UF membranes were turned into NF membranes, which exhibited a molecular-weight cut-off (MWCO) down to 890 Da with a high permeability of 32 $L{\cdot}m^{-2}{\cdot}h^{-1}{\cdot}bar^{-1}$. Furthermore, the MWCO was sequentially lowered down to 410 Da with another 20 cycles of deposition.

Alternatively, metal alkoxides were ALD-deposited on ceramic membranes, followed by calcination to transform the dense alkoxide films into microporous oxide layers atop the ceramic substrates, thus

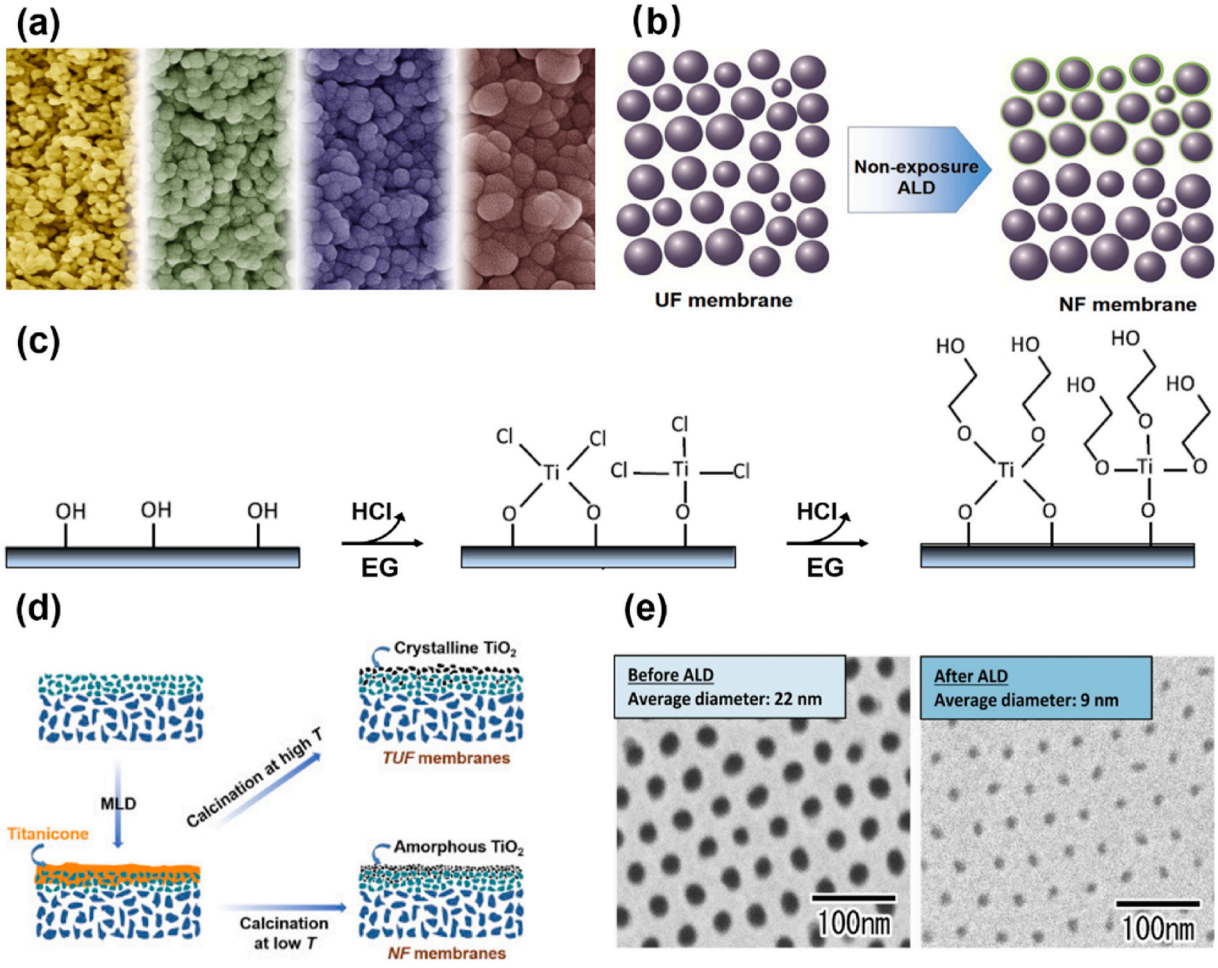

Fig. 8. ALD treatment of inorganic membranes. (a) Precisely tailored pore structures of ZrO_2 ceramic membranes by ALD-deposited Al_2O_3 [86]; (b) Diagram of using ALD to turn ceramic UF membranes into NF membranes by restricting the exposure time [87]; (c) Schematic diagrams of depositing titanium alkoxides on flat membranes and transforming into porous TiO_2 as new separation layers [53]; (d) The fabrication process of turning deposited titanicone into porous TiO_2 layer [88]; (e) The pore size of AAO membranes was reduced to single-nanometer level by ALD [98].

producing inorganic NF membranes. Song et al. [53] used $TiCl_4$ and EG as precursors to deposit titanicone (titanium alkoxide) onto anodized aluminum oxide (AAO) membranes, then calcined under 250°C to remove the organic parts of the titanicone and fabricated NF membranes (Fig. 8c). The pore size distribution of pristine AAO membranes was in the range of 20–50 nm and the growth rate of the titanicone was 0.42 nm per cycle, therefore, 60 cycles of titanicone deposition were enough to form dense coating layer on the AAO surface. Thus-prepared membranes showed no detectable PWF under the pressure of 7 bar for 24 h. After calcination, the 60-cycle-deposited AAO membranes showed a PWF 48 $L{\cdot}m^{-2}{\cdot}h^{-1}{\cdot}bar^{-1}$, which was much higher than polymeric NF membranes. The rejections of the membranes towards NaCl, Na_2SO_4, $MgCl_2$, and $MgSO_4$ were 29%, 43%, 24% and 35%, respectively. Also, Chen et al. [54] successfully turned the tubular ceramic membranes (pore size ~5 nm) into NF membranes by transforming the deposited titanicone into porous TiO_2 layers on the membranes. Furthermore, by changing the calcination temperature, the obtained TiO_2 can be controlled to be in the amorphous or crystalline state, thus giving different effective pore sizes in the NF and tight UF range, respectively (Fig. 8d) [88].

The photocatalytic function was endowed to ceramic membranes by ALD of semiconducting metal oxides. To enhance the anti-biofouling performance of ceramic membranes, a layer of ZnO (36.5 nm) was uniformly deposited into the nanopores of ceramic membranes [89]. After 200 cycles of ALD at 150°C, the ZnO exhibited good crystallization, which endowed the ceramic membranes with sufficient photocatalytic activity. After exposed to UV-A irradiation, ZnO would generate reactive oxygen species, which impeded the formation of biofilm. By choosing proper precursors, element doping or nanostructure construction was very easy to implement in ALD processes to promote the photocatalytic ability of deposited layers. Zhang et al. [90] used $TiCl_4$/water and $TiCl_4/NH_4OH$ as precursors to deposit TiO_2 and N-doped TiO_2 onto ceramic membranes, respectively. After doping with N element, a new band was formed in the bandgap of TiO_2. The N-doped ceramic membranes exhibited a red shift in the absorption of visible light, which endowed the membranes with 24 times higher photocatalytic efficiency than the uncoated one. Lee et al. [91] used $TiCl_4$/-water and $TiCl_4/NH_4OH$ alternatively deposited TiO_2 and N-doped TiO_2 hybrid layers on AAO and ceramic membranes. After deposited with the hybrid layers, the membranes were endowed with sunlight-activated photocatalysis, which degraded ~40% methyl orange under visible light (100 mW cm^{-2} of irradiance).

ALD has been frequently used to deposit nanoparticles of noble metals on ceramic membranes to prepare membrane reactors for chemical catalysis and gas separations. Lu et al. [92] adopted ALD to deposit Pd nanoparticles onto alumina ceramic membranes, thus forming a catalytic membrane exhibited excellent performance in the *p*-nitrophenol reduction to *p*-aminophenol. To further investigate the relationship between the membrane surface property and Pd deposition, four kinds of substrates, i.e. pristine ceramic membranes, TiO_2-deposited ceramic membranes with calcination (in pure Ar gas or H_2/Ar mixture gas (1:9 in volume)) and without calcination were used. Comparing with the Pd deposited on pristine ceramic membranes, the Pd content on the TiO_2-deposited membranes was increased significantly. After TiO_2 deposition and calcination in mixture gas, the loading amount of Pd was increased by 50% compared to the pristine ceramic membranes (14.1–9.7 mg m^{-2}). XPS results showed that the calcination process transferred the bulk-phase oxygen vacancies of the membranes to surface oxygen vacancies, and the H_2 atmosphere was beneficial for removing organic part of the Pd precursor to produce zero-valent Pd. Therefore, the TiO_2-deposited ceramic membranes calcinated in mixture gas were the best candidate for Pd deposition, which showed the highest conversion rate towards the reduction of *p*-nitrophenol after Pd loading. By changing the concentration of $NaBH_4$, the conversion efficiency reached 100% with excellent selectivity and acceptable stability. After coated with 10 nm TiO_2, the pore radius of γ-Al_2O_3 membranes was decreased to ~0.7 nm, and the permeance of hydrogen and carbon dioxide was reduced about one order magnitude (from 10^{-7} to 10^{-8} $mol{\cdot}m^{-2}{\cdot}s^{-1}{\cdot}Pa^{-1}$) [93]. With increasing temperature, the CO_2 and H_2 permeances of pristine membranes were both reduced. However, the CO_2 permeance was decreased and the H_2 permeance was increased after TiO_2 deposition. The different trends were ascribed to the negative and positive apparent activation energies of CO_2 (−6 kJ mol^{-1}) and H_2 (1 kJ mol^{-1}), respectively. Due to the inference of CO_2 molecules, the separation factor of H_2 towards CO_2 in the H_2/CO_2 mixture gas reached 5.8 at 448 K. In another study, the Pd cluster was deposited into the pores of γ-Al_2O_3 ceramic membranes under 220°C by using palladium hexafluoroacetylacetonate ($Pd(hfac)_2$) and formalin as precursors [94]. After 2000 cycles of deposition, the modified membranes exhibited high H_2 selectivity. Although the kinetic diameter of He molecules (2.60 Å) was smaller than the H_2 molecules (2.89 Å), the H_2 permeance of the membranes was higher than that of He in each test. This should be ascribed to the strong affinity between H_2 and Pd clusters, which formed PdH_x species to accelerate the transportation of H_2. The modified membranes exhibited permselectivities of ~23 and ~13 towards the H_2/N_2 and H_2/CO_2 gas pairs, respectively. Moreover, the H_2 permeance of the membranes was higher than 1100 GPU at 188°C, and the separation factors for H_2/N_2 and H_2/CO_2 gas pairs were ~16 and ~9, respectively.

It must be noted that AAO membranes featuring with uniform pore sizes, straight pore profiles and high porosity have been extensively used as model substrates to investigate the ALD process on porous membranes and also to reveal the structure-property relationship of ALD-deposited membranes [95–97]. The AAO membranes with single-nanometer pores were difficult to be prepared directly by the anodization method. However, their pore sizes could be progressively narrowed to the selected value with the help of ALD. Yanagishita et al. [98] used ALD to deposit Al_2O_3 or TiO_2 into AAO membranes and successfully tuned the pore size to the single-nanometer level. Benefiting from the merits of ALD, the pores with an aspect ratio of 1500 (45 μm in height and 29 nm in diameter) were deposited with uniform oxide layers (Fig. 8e). SEM characterization and N_2 adsorption tests showed that the pore size reduction was homogeneous through the entire thickness of the AAO membranes. Membranes with pore size lower than 10 nm were tightened by ALD at an average speed of 0.1 nm per ALD cycle. After 40 cycles of deposition, the pore size of the membranes was reduced from 10 nm to 6 nm. Vega et al. [99] even demonstrated that the permselectivity and transport parameters of AAO membranes with an aspect ratio up to ~2000 were effectively adjusted by depositing various oxides (e.g. Al_2O_3, SiO_2, and Fe_2O_3). Gelde et al. [100] deposited 6 nm TiO_2 onto two AAO membranes and reduced their pore size to 10 nm and 13 nm, respectively. Then, they used BSA (stokes radius = 3.48 nm) as probe molecules to analyze the relationship between membrane fouling and pore properties. They found that BSA preferred to foul the outer surface of small-pore membranes and the inner pore wall of large-pore membranes. Because of the two fouling modes, the fouled membranes showed different transmittance reduction in visible light region, and the changes in the optical property were supplementary information for membrane fouling analyses. Oh and coworkers demonstrated an interesting thickness-dependent crystallinity and surface energy of Y_2O_3 thin films ALD-deposited onto AAO membranes [101]. With lower film thickness (<10 nm), the amorphous phase was dominant in the Y_2O_3 film, and only some small crystallites appeared. As a result, the thin Y_2O_3 film showed high surface energy and a hydrophilic surface. As the thickness increased, crystalline “islands” emerged and the facets of (222) and (440) planes gradually appeared, which were expanded with the growth of Y_2O_3 film. The areal coverage of the crystalline structures maximized and kept unchanged with further increase in film thickness. During this process, the surface energy of the film was gradually decreased with WCAs increased from 45° to 100°. By utilizing the tunable surface energy of Y_2O_3 films conformally deposited on AAO membranes, the membranes were successfully used as tweezes to separate different liquid drops or as filters to separate 91% water from oil.

Romero et al. [102] employed ALD to deposit SiO_2 on AAO membranes. It was found that the ionic transportation of AAO membranes was obviously affected by the deposited SiO_2. On one hand, the SiO_2 layers on AAO surface and pore walls reduced the membrane pore diameter and porosity. On the other hand, the SiO_2 layers caused 75% decline of positive effective fixed charges on the AAO membrane surface. To analyze the influence of different depositing layers on the performance of membranes, Cuevas et al. [103] deposited four metal oxides (Al_2O_3, ZnO, TiO_2 and Fe_2O_3) onto AAO membranes (pore size = 12 ± 2 nm, porosity = 12–15%). After coated for 5–7 nm metal oxides, the pore size and porosity of the porous alumina substrates were decreased by 30% and 50%, respectively. The AAO membranes exhibited different optical characteristic parameters after coated with different oxides. The bandgap of the membranes was significantly reduced after deposited with several nanometers of Fe_2O_3. Meanwhile, due to the comparable pore size and porosity, the permselectivity of deposited membranes towards electrolytes was dominated by surface properties, which were comprehensively considered as membrane potentials. The ZnO- and Al_2O_3-coated membranes exhibited similar and more negative membrane potentials, therefore, thus-prepared membranes showed identical permselectivities and were better than others. Furthermore, metals, semiconducting oxides have also been deposited on AAO membranes to render membranes new functions such as (photo)catalysis and antimicrobial activity [95,104,105]. Chen et al. [105] deposited TiO_2 on the AAO membranes as the intermediate layer, then thermally annealed the deposited membranes to crystallize the TiO_2 layers. Subsequently, Pt nanoparticles (1–5 nm) were deposited on the pore wall of deposited AAO membranes to form Pt@TiO_2 structures. When the methylene blue solution flowed through thus-modified AAO membrane, the confined space made the collision between reactant and catalyst more frequently. Consequently, with the help of high photocatalytic reactivity of Pt@TiO_2 structures, the modified membranes showed better removal efficiency towards methylene blue under UV light illumination.

In addition to industrially used ceramic membranes and model AAO membranes, other inorganic membranes made from various materials such as metals [106,107], silicon [108], carbon nanotubes (CNTs) [109,110] have also been modified or endowed with new functions by ALD. An interesting example is using ALD to build protection layers on perovskite membranes by taking advantage of precise control in deposition thickness [111]. To protect the $La_{0.6}Sr_{0.4}Co_{0.2}Fe_{0.8}O_{3-\delta}$ (LSCF) membranes from the sulphur poisoning, Zhang et al. deposited a layer of Al_2O_3 on the membrane surface. The authors found that the thickness of Al_2O_3 layers was an extremely important factor for the protection of LSCF membranes. The critical thickness for the Al_2O_3 layers was ~30 nm. Thicker Al_2O_3 layers would greatly impede the O_2 permeation while thinner Al_2O_3 layers showed weak protection for the sulphur poisoning.

7. ALD of polymers on inorganic and polymeric membranes

Polymers including polyimide (PI) and PA which are common membrane-forming materials can also be synthesized via ALD, thus forming a modification layer or even the selective layer for a substrate membrane. ALD of polymers uses two organic monomers as the precursors, restricting the step polycondensation between vaporized precursors on the substrate surface. This niched ALD process is specifically termed as molecular layer deposition (MLD), which is a branch of the ALD technology, and the most significant difference between MLD and ALD is the precursor type. In ALD, the widely used precursors are metal precursors (e.g. $TiCl_4$, $Al(CH_3)_3$, and $Zn(CH_2CH_3)_2$) and non-metal precursors (e.g. H_2O, O_3, NH_3, and H_2S). In MLD, one of the two precursors or both two precursors are bifunctional metal-free organics, which are used to deposit hybrid materials (e.g. depositing metal alkoxides) or pure polymers. A layer of molecules is deposited after one MLD cycle, and the molecular layer is usually several times thicker than the atomic layer. Sheng et al. [47] adopted ethylenediamine (EDA) and pyromellitic dianhydride (PMDA) as precursors to deposit PI on PES membranes. As shown in Fig. 9a, the deposited PI formed conformal and uniform layers on all parts of PES membranes, and the pore size of PES membranes reduced obviously after deposition. The rejection of PES membranes (modified with 3000 cycles of MLD) towards 23-nm silica nanospheres increased from none to 60% and the flux was decreased by ~54%. Due to excellent mechanical and thermal stabilities of PI, the physical stability of PES membranes was improved after deposition. The deposited PI layer was further crosslinked in EDA solutions and the overall performance of the deposited PES membranes was greatly enhanced [112]. Due to the further reduced pore size, the thus-prepared PES membranes retained more than 90% of 12-nm SiO_2 nanospheres. The permeability, fouling and corrosion resistance of the modified membranes were also enhanced after crosslinking. Although the PI had been successfully deposited on PES membranes, the high deposition temperature (160°C) still restricted its applications on temperature-sensitive polymeric membranes. To expand the application of PI deposition, Xiong et al. [113] lowered the deposition temperature down to 110°C and successfully deposited PI on chemically inert PP membranes. After 250 cycles of deposition, the wettability of PP membranes was slightly enhanced and the water flux of the membranes increased by 25% at no expense of the selectivity. In a further work, PI was deposited onto AAO membranes with selected depths by controlling the precursor exposure time [114]. As shown in Fig. 9b, the PI deposition was limited to the surface in the short-exposure mode, and was penetrated into the pores in the long-exposure mode. Both modes improved the separation performance of AAO membranes, and the membranes deposited with 50 cycles at the short-exposure mode exhibited the best BSA rejection (from 0 to 82%).

Creating thin separation layers on porous substrates by MLD is a promising strategy to prepare new composite membranes. However, the vaporized precursors would filtrate into the pores thus forming dense deposition layers and significantly reduced the permeability of modified membranes. To solve this problem, Welch et al. [115] used plasma-assisted ALD (PA-ALD) to deposit a dense layer of Al_2O_3 onto substrates as capping layers applying TMA and oxygen radicals as precursors, then used *m*-phenylenediamine (MPD) and trimesoyl chloride (TMC) as precursors to deposit PA films on the Al_2O_3 layer. Finally, the composite membranes were etched from the backside to remove the Al_2O_3. Due to the short lifetime of oxygen radicals, Al_2O_3 tended to deposit on membrane surface rather than in pores, thus the deposited Al_2O_3 layer was particularly suitable for working as a capping layer to mediate the PA layer and the substrate. Due to the different thermal expansion, the Al_2O_3 layer on PES membranes was fractured during the deposition of PA at 130°C. Interestingly, the PA film was anchored to the PES membrane surface through the fractures in Al_2O_3 layer, which avoided peeling the PA layer off the PES substrates. Therefore, with increasing of cracks on the Al_2O_3 layer, the composite membranes exhibited better robustness. Many other polymers, such as polyazomethine (PAM) [116], poly(3,4-ethylenedioxythiophene) (PEDOT) [117], polyuria (PU) [118], even the PI-PA hybrid [119], have been successfully deposited by MLD. Although these polymers have already been used in a diversity of applications, there are still some challenges such as unstable chemical structure and high deposition temperature, restrict their applications in membrane modification. Once these polymers can be deposited on membranes, some new microstructures and functions may be realized and expand the utilization scopes of the deposited membranes.

8. ALD for emerging membranes

Recently, emergent materials such as graphene and graphene oxide (GO), MOFs, polymers of intrinsic microporosity (PIMs), and hexagonal polymorph boron nitride (*h*-BN) have attracted increasing attentions as building blocks to prepare new-generation membranes [120–122]. These emergent materials are featured with two-dimensional structures and/or intrinsic nanopores built in their molecular frameworks.

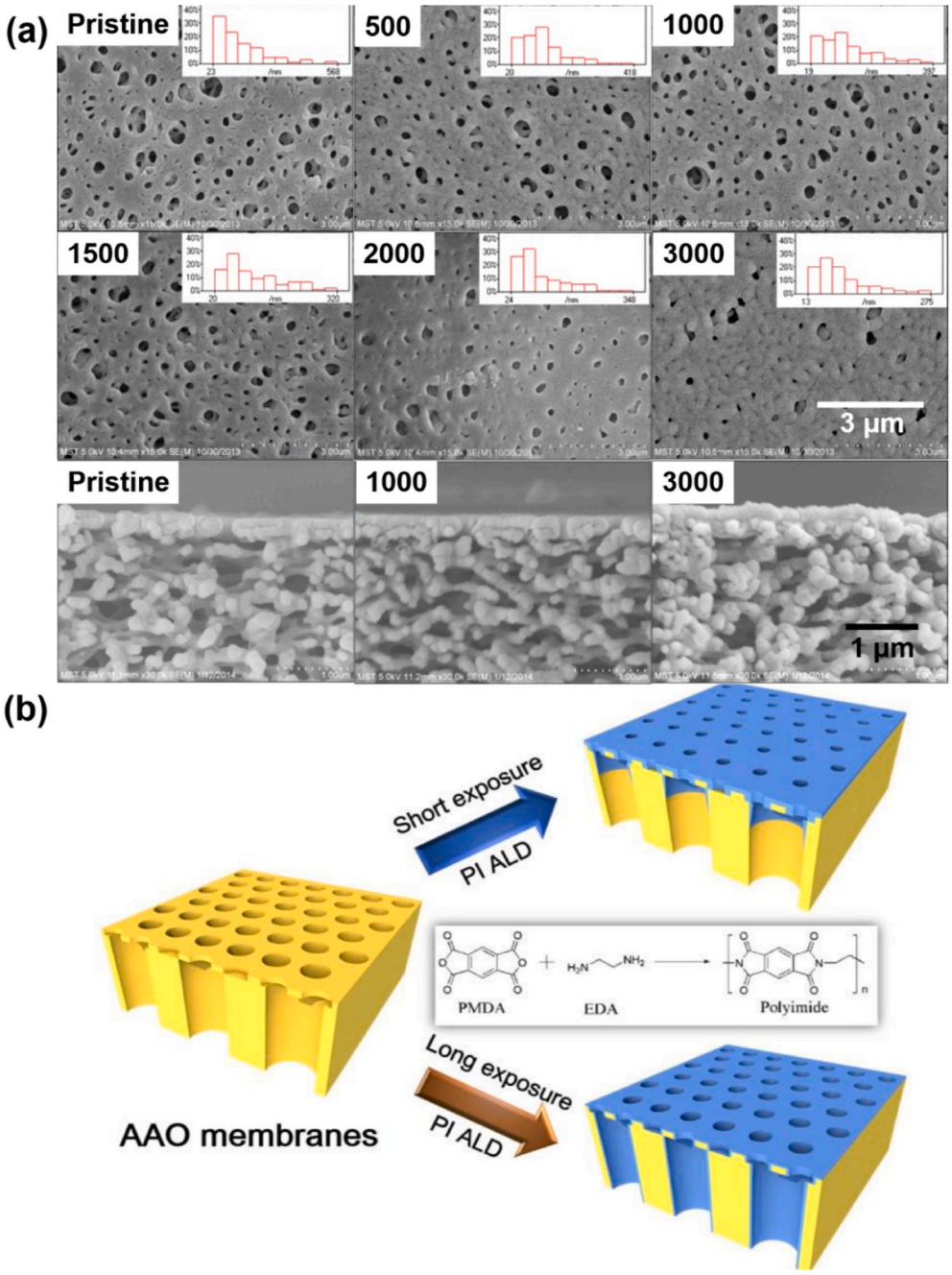

Fig. 9. ALD of polymeric materials to modify polymeric and inorganic membranes. (a) Surface and cross-sectional SEM images of pristine and deposited PES membranes [47]; (b) Schematic diagrams of PI deposition on the alumina membranes in the mode of long and short exposure [114].

Table 3
ALD-enabled modification, functionalization, and synthesis of emergent materials and their membranes.

Emergent materials	Deposited materials	The way of using ALD	Applications	Ref.
GO	Al_2O_3	Al_2O_3 depositing on the outmost GO surface and healing defects	Desalination by NF	[57]
GO	Al_2O_3	Al_2O_3 forming uniform layers on GO surface	Moisture barrier	[123]
PIM	Al_2O_3	Al_2O_3 coating along the micropores of PIM	Gas separation	[124]
ZIF	ZnO	ALD of ZnO as the precursor layer for subsequent synthesis	–	[125]
			–	[126]
			Gas separation	[55]
			Gas separation	[56]
MIL-53-NH_2	Al_2O_3	ALD of Al_2O_3 as the precursor layer for subsequent synthesis	–	[126]
UiO-66	UiO-66	Direct synthesis	–	[127]
UiO-66 derivatives	UiO-66 derivatives	Direct synthesis	Luminescence and antibiosis	[128]
h-BN	*h*-BN	Direct synthesis	Ion transportation	[129]
SiO_2	Bilayer 2D SiO_2	Constructing bilayer structures	Gas separation	[130]

Membranes made from them possess well-organized transport paths with uniform geometries and customized surface chemistry, ensuring fast permeation and tight rejection. Like the applications in traditional polymeric and inorganic counterparts, ALD also has strong capability to modify/functionalize or even directly synthesize new membranes of these emergent materials. One of the most desirable advantages of the new membranes is their distinguished pore uniformity, therefore, ALD is particularly suitable for the adjustment of their pore sizes and pore-wall chemistry as the pore uniformity will be maintained to the largest extent after ALD treatment. There are a number of works reporting the ALD-enabled modification, functionalization, and synthesis of these emergent materials and their membranes, which are listed in Table 3.

ALD showed different deposition modes on graphene and GO due to their different chemical structures [123]. For instance, Al_2O_3 tended to nucleate at the defect of graphene while formed uniform films on the GO surface. Choi et al. integrated Al_2O_3 and GO together and formed "$Al_2O_3(GO/Al_2O_3)_n$" (n = 1, 2, 3) structures by depositing different thickness of Al_2O_3 on the GO surface to fabricate moisture barriers. The pure GO layer showed no barrier ability towards moistures. However, the composite $Al_2O_3(GO/Al_2O_3)_n$ structures showed moisture permeations of 2.03, 1.94, and 1.81 $\times 10^{-4}$ g m^{-2} day^{-1} when n = 1, 2, and 3, respectively. The compounded GO provided tortuous paths and the following ALD processes narrowed the pore size of GO layers, therefore, the inserting of GO enhanced the moisture barrier property of Al_2O_3. Kim et al. [57] stacked GO nanosheets to prepare NF membranes first, and then used plasma-enhanced ALD (PEALD) to deposit few cycles of Al_2O_3 onto the outmost layer of thus-prepared membranes. After deposition, the GO membranes showed simultaneous increment in the permeability and selectivity towards NaCl solution. During the deposition, TMA and oxygen plasma were used as precursors. The –CH_3 groups were combusted with oxygen plasma to form CO, CO_2 and H_2O, and then reacted with the produced H_2O to form –OH groups [131]. After 9 cycles of deposition, the C/O ratio of the GO membrane surface was lower than 1, which confirmed the successful deposition of the Al_2O_3. Moreover, the WCA of the membrane was decreased from ~70° to ~40°. The GO membranes treated with oxygen plasma showed better permeability because of the devastating effect from energetic particles, while the selectivity was undermined with the damage of the membrane structure. After introducing TMA, the GO reacted with TMA first, especially the defects on the GO surface, and then the adsorbed TMA reacted with the oxygen plasma to form Al_2O_3. Therefore, the membrane structure was reserved and even some defects on the GO surface were healed by Al_2O_3, which enhanced the permeability and selectivity of the GO membranes. The permeance of deposited GO membranes was increased from 32.9 to 68.0 L·m^{-2}·h^{-1}·bar^{-1}, and the rejection towards NaCl was increased from 46.7% to 63.8% (Fig. 10a).

PIMs are amorphous polymers constructed by rigid and contorted backbones. The packing of PIM chains is inefficient and interconnected pores are thus formed [132]. Because of the small pore size, PIMs were hard to be modified by conventional methods. To enhance the gas separation ability, Chen et al. [124] used TMA (5.4 Å) as precursor to deposit Al_2O_3 into the PIM-1 pores (<14 Å) (Fig. 10b). The nucleation of Al_2O_3 occurred predominantly on the –CN groups of the PIM-1 and the nucleation was completed after 6 cycles of Al_2O_3 deposition (noted as PIM-1-Al_2O_3-6). The pore size of PIM-1-Al_2O_3-6 was mainly concentrated around 6.2 Å, while the pore size of other membranes showed bimodal distribution and at least one of the regions was greater than 6.2 Å. As a result, the PIM-1-Al_2O_3-6 membrane showed the best separation

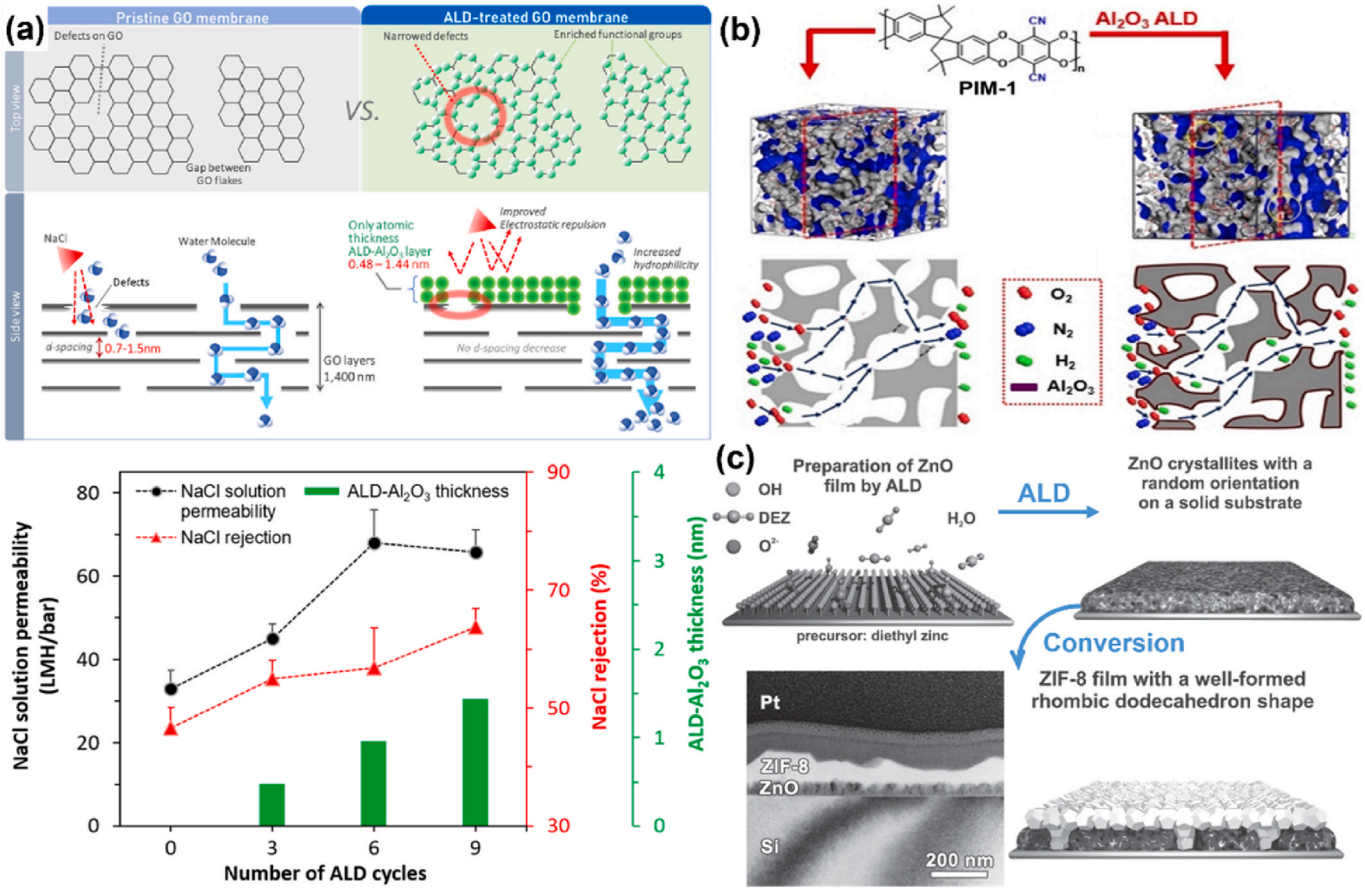

Fig. 10. Synthesis of emergent separation materials by ALD. (a) The simultaneous increments of GO NF membranes after PEALD and the mechanism of thus-prepared membranes for salt removal [43]; (b) The chemical structure, 3D structures and the separation performance of pristine and deposited PIM-1 [124]; (c) ALD-deposited ZnO layers are used to synthesize ZIFs. The TEM result shows that the deposited metal oxides layer is not fully converted into ZIFs [125].

performance. Thanks to the narrowed pores and uniformed pore size distribution, the strong molecular sieving effect greatly promoted the permeability of PIM-1-Al_2O_3-6, and excellent selectivity was obtained because of the diffusivity selectivity. The performance of the PIM-1-Al_2O_3-6 membrane for H_2/N_2, O_2/N_2 and H_2/CH_4 separations was higher than the trade-off line of 2015, and the separation performance of CO_2/CH_4 was approaching the trade-off line of 2019. Moreover, the thermal, mechanical and long-term stabilities of PIM-1 were enhanced with the deposition of Al_2O_3.

MOFs are synthesized from organic linkers and metal nodes, and metal oxides such as Al_2O_3, ZnO, and ZrO_2 can be used as the metal sources. As these oxides can be easily coated on various substrates by ALD, there are extensive works using ALD-deposited ZnO, Al_2O_3, and ZrO_2 as metal sources to synthesize different MOFs. In this strategy, ZnO was most commonly ALD-deposited on different substrates, and then reacted with organic linkers in solutions to form zeolitic imidazolate frameworks (ZIFs) [125,126,133–135]. Khaletskaya et al. [125] demonstrated that 1 nm of the ALD-deposited ZnO layer could be turned into 21.2 nm of the ZIF-8 layer (Fig. 10c). In this case, ~21% thickness of the ZnO layer was consumed, forming ZIF-8 during the synthesis processes. As for the ALD-deposited Al_2O_3 and ZrO_2, they were turned into $[Al(OH)(1, 4\text{-ndc})]_n$ and UiO-66, respectively. Bechelany et al. [126] deposited uniform ZnO and Al_2O_3 layers on electrospun polyacrylonitrile (PAN) nanofiber membranes as metal sources to synthesize homogeneous ZIF-8 and MIL-53-NH_2 layers, respectively. Under different reaction conditions, the conversions of ZnO and Al_2O_3 varied from 86% to 96% and 61% to 94%, respectively. In the synthesis of MOFs, the organic linkers helped the oxides dissolving into solutions to form ions first, and then reacted with the ions to form MOFs. With thicker MOFs layers, the diffusion of organic linkers into bulk volumes became retarded, so part of the oxides was unreacted and the conversion efficiency was lower than 100%. Comparing with the conventional solvothermal synthesis, ALD-deposited metal oxide layers generate MOFs in a "dissolving-reacting" mode, which can provide slower growth rates, conformal and continuous structures. This makes the MOFs layer more suitable for separation processes. Drobek et al. [55] deposited ZnO into the macropores of ceramic supports and turned them into ZIF-8 nanocomposite membranes by solvothermal synthesis. The performance of the nanocomposite membranes was controlled through precisely adjusting experiment parameters. The membranes extracted H_2 from H_2/CO_2 or H_2/CH_4 gas mixtures (1:1 mol ratio, 100°C) with selectivities of ~7.8 and ~12.5, respectively. Ma et al. [56] fabricated ZIF-8 membranes through ALD and ligand-induced permselectivation. Porous alumina membranes with mesoporous γ-alumina layer (2–5 nm thick) were used as substrates. After ZnO deposition, the Zn element was distributed evenly in the γ-alumina layer. Then ZnO (>20 cycles) reacted with 2-methylimidazole vapor and turned into ZIF-8. According to the element distribution result, the generated ZIF-8 layer was centered around the top surface of γ-alumina layer, which formed new separation layers. Comparing with other methods to synthesize MOFs membranes, this "pore blocking–converting" strategy confined the reaction exclusively in the ZnO-blocked pores, which avoided the defects and nonselective grain boundaries in the common methods. As a result, the membranes exhibited exellent propylene permeance (0.01–0.06 $mol{\cdot}m^{-2}{\cdot}s^{-1}$) and propylene/propane selectivity (~50–70) under the feed pressure of 1–7 atm.

In addition, ALD can also be used to directly synthesize some emergent materials with intrinsic porosity. Some MOFs, for instance, UiO-66, has been directly synthesized by ALD as their organic linkers and metal sources are reasonably volatile. Lausund et al. [127] adopted 2-amino-1, 4-benzenedicarboxylate and $ZrCl_4$ as precursors to directly deposit amino-functionalized UiO-66 thin films. They further used organic linkers with different chain lengths to tune the pore sizes and porosity of the ALD-deposited MOF films [128]. Another case is the *h*-BN which has a spacing of 0.333 nm between layers and a distance of 0.25 nm between each borazine ring center [136]. The *h*-BN showed a uniform honeycomb structure and strong hydrophobicity. It has been confirmed that ALD is effective to deposit uniform *h*-BN films into different substrates [137–139]. For instance, Weber et al. [129] used BBr_3 and NH_3 to deposit *h*-BN films on different substrates and confirmed the conformality of the deposited films. It can be expected that if the UiO-66 or *h*-BN thin films are ALD-synthesized on macroporous supports they will work as fast and highly selective membranes for gas separation and desalination. It should be noted that the direct ALD synthesis of membranes of MOFs or other materials with intrinsic porosity is somewhat overlooked, however, we believe it will rise soon because of its great potential in affording fast and selective separation of molecules and ions. Here, we summarize the three different ways to construct microporous selective layers on macroporous substrates by ALD we discussed in Section 3.3 and Section 8 in Fig. 11.

With ever-growing interests in ultrathin 2D membranes, ALD is receiving more attentions because of its strong capability to synthesize atomic or molecular layers of various materials of different chemical nature. These ultrathin layers are expected to show unprecedented transport behaviors, thus enabling the design and preparation of next-generation membranes. There is a very recent report on the unusual transport behaviors of an ALD-synthesized 2D material. Naberezhnyi et al. [130] ALD deposited 6 cycles of SiO_2 onto the Au/mica substrates under 240°C. After annealing in air and transferring onto Si_3N_4 windows, a vitreous bilayer 2D SiO_2 membrane was successfully prepared (Fig. 12). The transportation mechanism of thus-prepared membranes was different from the size exclusion principle. The permeation rate of the He gas at room temperature was 1.5×10^{-8} $mol{\cdot}m^{-2}{\cdot}s^{-1}{\cdot}Pa^{-1}$, which was several magnitudes lower than that of D_2O, C_3H_7OH, and $C_4H_9C(O)CH_3$ (4.5×10^{-5}, 1.7×10^{-5}, and 1.9×10^{-4} $mol{\cdot}m^{-2}{\cdot}s^{-1}{\cdot}Pa^{-1}$, respectively). According to the density functional theory calculation, $C_4H_9C(O)CH_3$ showed the adsorption energy of 57.3 kJ mol^{-1}, which was higher than D_2O and C_3H_7OH. Therefore, the chemical affinity between the molecules and membranes showed stronger important influence on the membranes with small pores approximating to the size of gas molecules.

9. Innovative ALD devices and processes

ALD is regularly working in the temporal mode, and material deposition cannot be continuously performed, thus significantly hampering the efficiency and productivity. Recently, some research efforts have been made to innovate ALD devices and processes to enhance the ALD productivity and to expand the application fields of ALD. Spatial atomic layer deposition (SALD) is distinguished from these efforts and is highly promising to become an industrialized continuous ALD process with high productivity. Different from the temporal ALD, the precursors used in the SALD system are separated by locations rather than by deposition sequences. As shown in Fig. 1b–c and Fig. 13a, in the temporal ALD, the precursors are sequentially pulsed into the reaction chamber and separated by purge steps. In SALD, two precursors are spatially separated by inert gases (Fig. 13a). Both the transportation of precursors and the status of substrates in two ALD systems are different. The substrates in the temporal ALD are fixed in the reaction chamber while the substrates and precursor regions are keeping relative movement in the SALD system. The deposition cycle is completed by repeating pulse-purge steps and relative movement in the temporal ALD and SALD, respectively [140]. This novel SALD strategy makes ALD a continuous production process and provides two orders of magnitude faster production rate than the temporal ALD at maximum. Moreover, SALD frees the whole process from high vacuum conditions, which greatly reduces the equipment cost of the whole system and makes the atmospheric pressure ALD possible. As shown in Fig. 13b–d, different SALD devices have been invented, mainly including the roll-to-roll (R2R) SALD system, the rotating cylindrical SALD system, and the "close-proximity" SALD system [141–143]. Specifically, the R2R SALD system is generally designed for flexible substrates which repeatedly

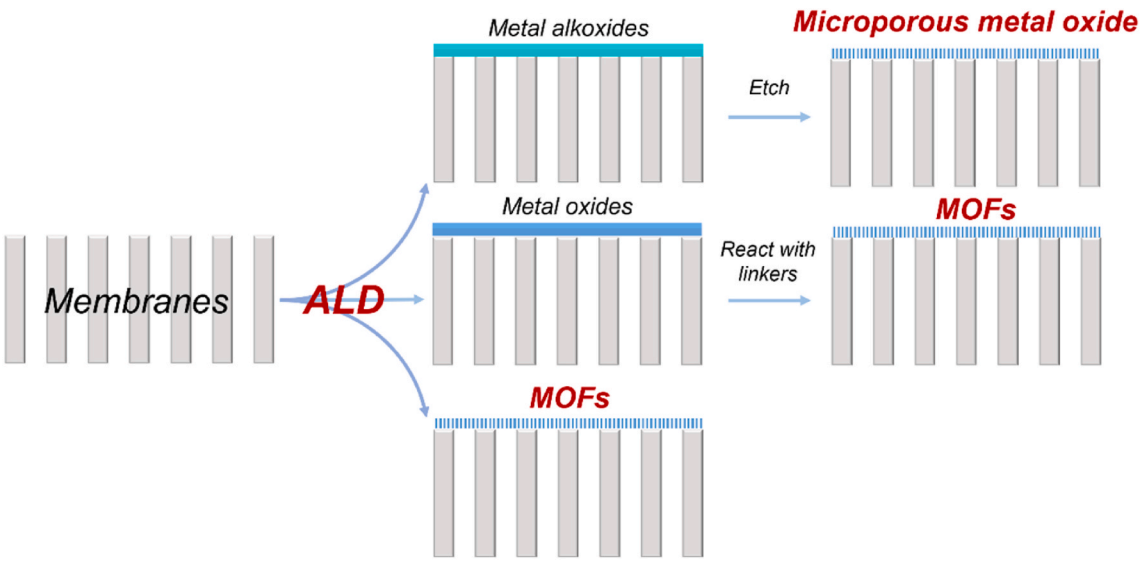

Fig. 11. Diagram of using ALD to build new separation layers on porous substrate membranes. (a) Etching metal alkoxides to form porous metal oxides; (b) transforming deposited metal oxides into MOFs; (c) direct ALD synthesis of MOFs.

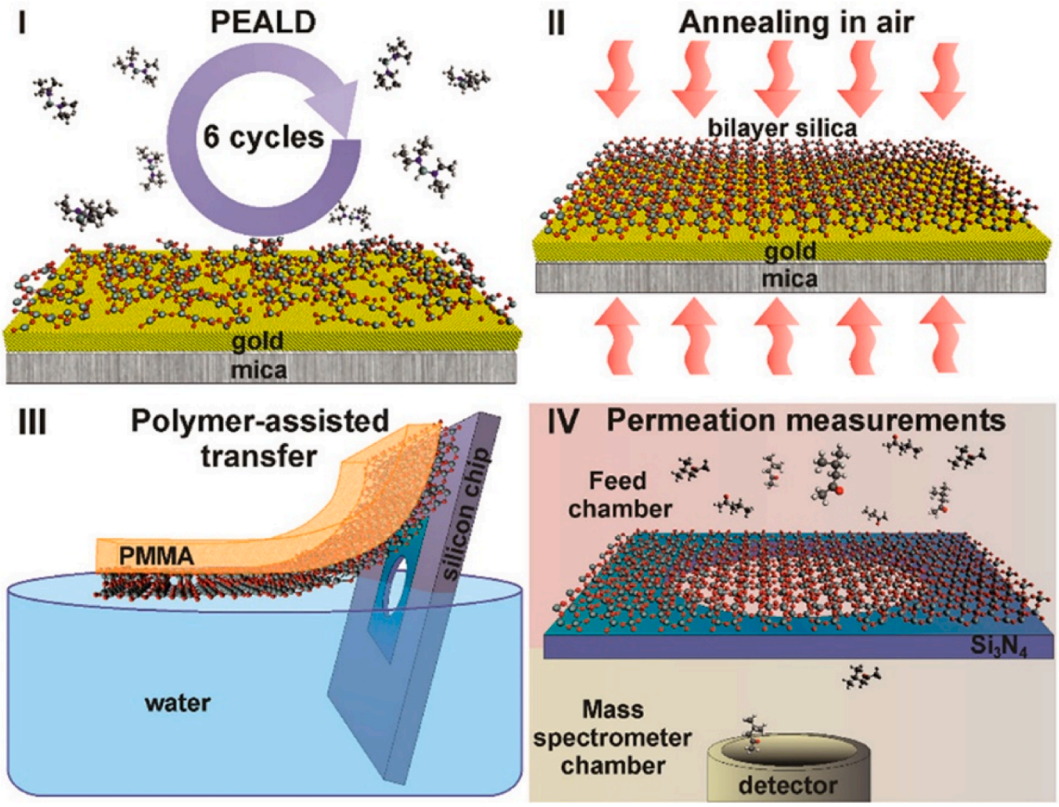

Fig. 12. Schematic of experimental procedures for ALD-synthesized ultrathin SiO_2 membranes [130].

shuttle between two precursor regions. The rotating cylindrical SALD system consists of two concentric rollers, and the gap between the rollers is used as the reaction chamber. The "close-proximity" SALD system is a showerhead-type device having parallel gas slots to spray inert gas or precursors.

Lee et al. [144] invented a R2R atmospheric atomic layer deposition (AALD) device, which was used to deposit uniform Al_2O_3 on both sides of commercial polyolefin Celgard separators and realized the continuous production. The precursors were sprayed out from a multi-slit gas source head, and the flow speed of carrier gas (nitrogen) for TMA and water was 700 and 1000 standard cubic centimeter per minute (SCCM), respectively. To avoid the intermixing of the two precursors, nitrogen flowing with a higher rate of 1220 SCCM was used as "walls" to separate TMA and water. Moreover, the nitrogen flows were also acted as purge steps when the substrates passed through. The gas head was consisted of dozens of slits. The movement of Celgard substrates was perpendicular to the gas head and the distance between the two components was less than 500 μm. A 5-cycle deposition was accomplished when the

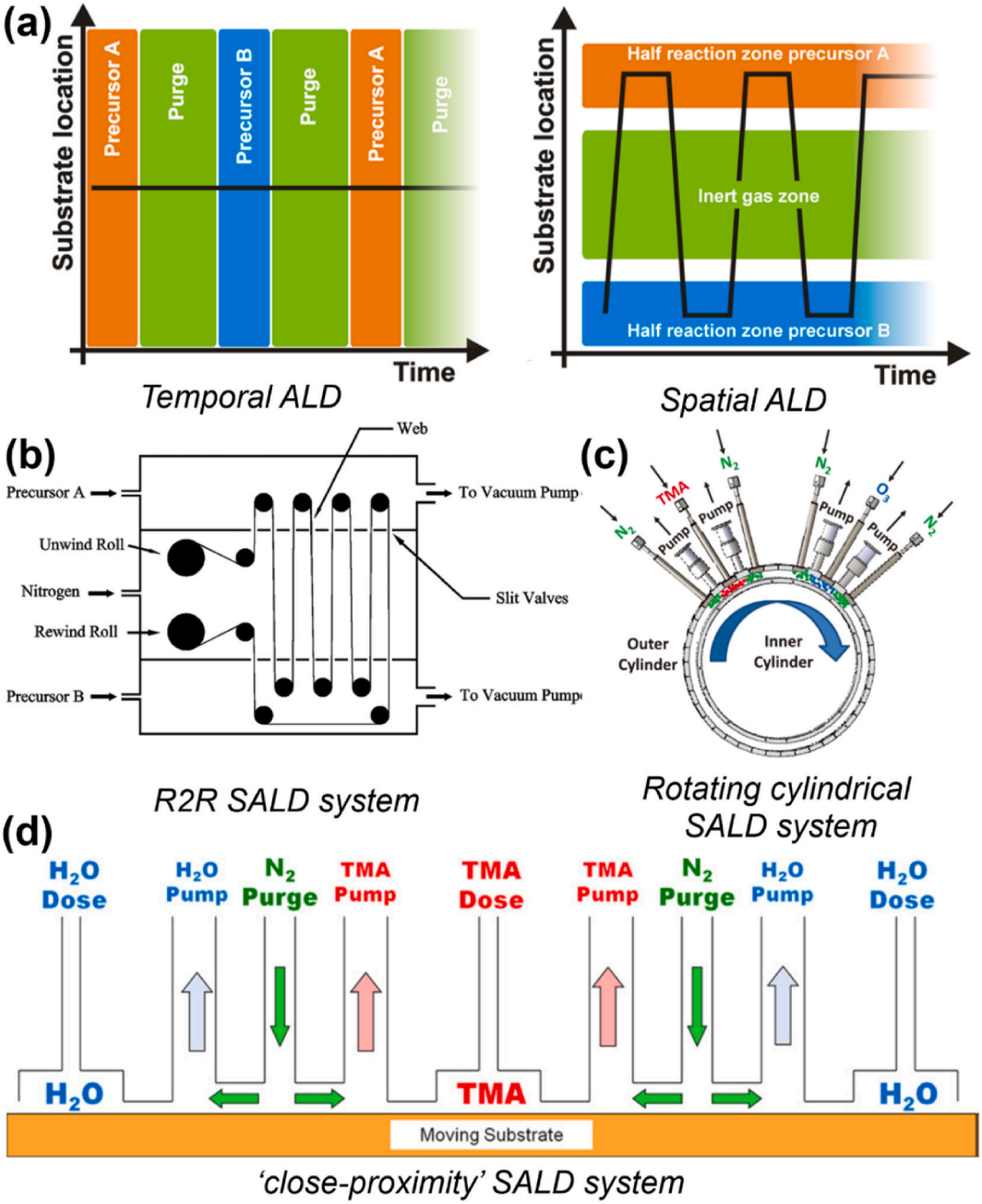

Fig. 13. ALD processes and devices working in different modes. (a) Scheme of processes [140]; (b) The R2R SALD system [141]; (c) The rotating cylindrical SALD system [142]; (d) The "close-proximity" SALD system [143].

membrane passed by the whole head every time. After the membrane passed the gas head for 30 times, 150 cycles of Al_2O_3 deposition were finished and ~5 nm Al_2O_3 layers were deposited on both side of the membranes. Only a negligible porosity decrement was detected (from 54% to 48%.), while the thermal and mechanical stabilities of the membranes were significantly enhanced, and the functionalized membranes showed enhanced affinity to electrolytes. Based on these improvements, the cells using these ALD-deposited membranes as separators exhibited better stability (~85% capacity retention) than the cells with pristine separators (~70% capacity retention) in cyclic performance tests. It is no doubt that such an R2R ALD device and process can be extended to continuously modify/functionalize other polymeric membranes. AALD has also been employed to deposit inorganic substrates with high efficiency. Hsu et al. [145] used AALD to deposit Al-doped ZnO films onto glass substrates. To simplify the doping processes, the TMA and DEZ precursors were simultaneously sprayed out the injector and co-introduced into deposition processes. As other AALD devices, N_2 was used as the carrier gas, purge gas and gas curtains. The substrates were perpendicular to the injector and the distance was 0.3 mm. When the deposition started, the substrates passed the injector back and forth with a speed of 150 mm s^{-1}. The processing time of one cycle in this AALD device was 3 s and its growth rate was 0.94 Å per cycle, which were 20 times faster and 3 times higher than the processing time (~1min) and growth rate (0.3 Å per cycle) in thermal ALD processes, respectively.

Moreover, AALD has great potential to produce ceramic NF membranes. Usually, ceramic NF membranes are fabricated by the sol-gel method. The membranes need to be coated for multiple times to narrow the pore sizes and achieve better selectivity. Consequently, ceramic NF membranes usually have thick separation layers, leading to lower

water flux [146]. To prepare highly permeable NF membranes, Shang et al. [147] used AALD to deposit TiO_2 on ceramic substrates for the purpose of reducing the pore size. The obvious feature of AALD was that the vacuum system was replaced by N_2 flow system to satisfy the self-limiting property of ALD processes. The pore size of the pristine NF membranes was narrowed from 0.7 nm to 0.5 nm within only three cycles of deposition. Thus-deposited ceramic NF membranes exhibited a MWCO between 260 and 380 Da, and a water permeance of 11–16 $L{\cdot}m^{-2}{\cdot}h^{-1}{\cdot}bar^{-1}$ which was higher than many commercial NF ceramic membranes. It was worth noting that the growth rate of TiO_2 in the AALD was 0.39 nm per cycle, which was higher than that in the temporal ALD. In another work, Liu et al. [148] designed a vertical forced-flow ALD device to obtain uniform coating on three-dimensional substrates including hollow-fiber membranes and increase the output. in this ALD device the precursors were pulsed from the top of the reaction chamber, then flowed through the cylinder reactor forced by the evacuation system (at the bottom of the reaction chamber). This system allowed the precursor permeating into the substrates quickly and uniformly, which resulted in effective production of conformal metal oxide coatings. No obvious difference could be detected after 400 cycles of TiO_2 deposition on the top, middle, or bottom parts of hollow-fiber membranes, demonstrating the uniformity of the deposited layers. By placing conduit plates into the forced-flow ALD devices, the "soak" function (as the exposure step in the temporal ALD) was added into vertical forced-flow ALD equipment [149]. This strategy prolonged the stay time of precursors in the reaction chamber, which coated more uniform deposition layers on the hollow-fiber membranes. Unfortunately, the separation performance of thus-deposited hollow-fiber membranes was not evaluated in these works.

In addition to design new ALD devices, innovation in the deposition process operated in regular ALD devices may also enhance the capability of ALD modification/functionalization of membranes. For instance, sequential infiltration synthesis (SIS) is a modified ALD process with particularly long exposure time. In SIS, the first precursor is holding in the reaction chamber for a long time, which allows it to diffuse into the bulk volume of substrates and react with the functional groups in the substrates (e.g., the TMA can react with the carbonyl groups to form Al–O–C bonds) [150,151]. Different from the regular ALD process deposition happens exclusively on the surface or subsurface regions, SIS occurs in the whole part of the substrates (including pore walls and solid phase of the substrates). To compare the difference between regular ALD and SIS on membrane modification, Waldman et al. [152] adopted both strategies to modify PES UF membranes by deposition of Al_2O_3. The water fluxes of ALD and SIS modified PES membranes were both reduced. Results from energy dispersive spectroscopy (EDS) showed that the Al element was detected through the whole PES membrane after SIS modification and only around the near surface region in the ALD-modified one. The flux reduction of ALD-modified membranes was caused by the constriction in the size of pore mouths, while the flux reduction of the SIS-modified membranes was caused by the constriction of the pore itself. These results reveal that under similar conditions ALD and SIS mainly act on the near surface region and entire volume, respectively. Moreover, the Al_2O_3 loading amount after 3 cycles of SIS was equal to the loading amount after 50 cycles of ALD, implying that SIS was more effective to load materials into the membranes. By taking advantage of the affinity between organometallic precursor and polar blocks of the polystyrene-*block*-poly(4-vinylpyridine) (PS-*b*-P4VP), Zhang et al. [153] combined SIS, ALD, and silane coupling together to

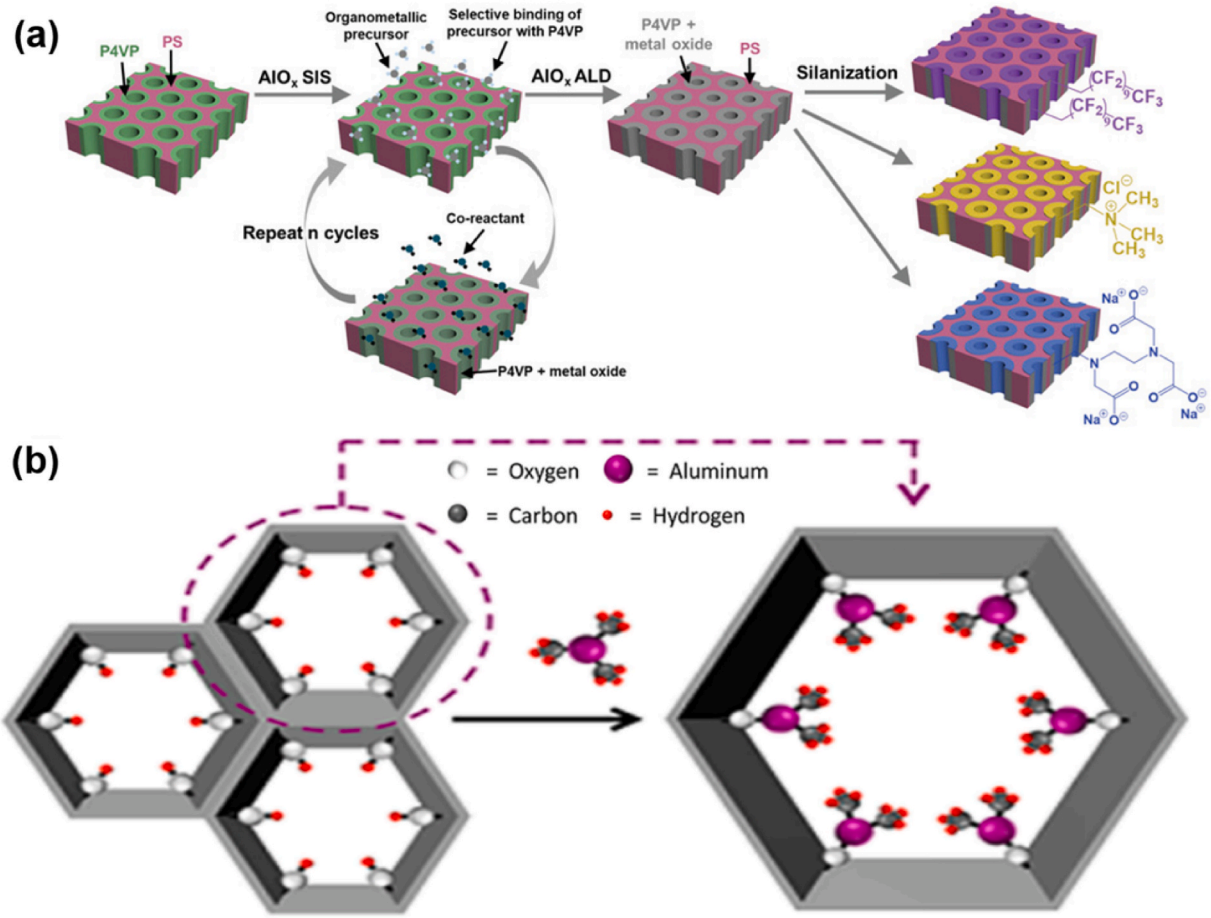

Fig. 14. New processes to perform ALD on membranes and MOFs. (a) The fabrication process of organic/inorganic/organic (PS-*b*-P4VP/deposited Al_2O_3/silane agents) isoporous membranes [153]; (b) Illustration of MOF metallation by semi-ALD modification [154].

fabricate organic–inorganic–organic isoporous membranes (Fig. 14a). The first SIS step was significant for the whole modification. Firstly, the metal oxide-P4VP interface formed in the SIS step would greatly promote the following ALD processes. Secondly, the pore size reduction of SIS was more effective. The pore size of pristine isoporous membranes was decreased by ~12 nm after only 3 cycles of SIS, while it required 30 to 40 cycles of ALD to achieve the similar result. After 3 cycles of SIS and 75 cycles of ALD, the membranes with original pore sizes of 38 nm and 55 nm showed a pore reduction of ~20 nm and ~22 nm, respectively. Moreover, the thermal stability and wettability of both membranes were enhanced. By using different silane coupling agents, the membranes were functionalized with fluorinated, cationic, and anionic surfaces. Combining the pore size reduction and specialized pore properties, membranes with sub-20 nm pores could fractionate proteins with similar sizes (3–4 nm) and separate small organic molecules (1–2 nm) from the mixtures with high selectivity and permeability.

Importantly, the semi-ALD process should be stated because of its great potential in fast modification of membranes with small pores. Typically, ALD involves alternative exposure of the substrates to two precursors. However, in some cases, only one precursor was pulsed into the reaction chamber to react with the substrates followed by inert gas purging, which is termed as "semi-ALD". In semi-ALD, the precursors diffuse into the fine pores in the substrates and react with the surface groups on the pore walls in the self-limiting way, thus forming a monolayer of precursor skeleton covalently bonded to the pore wall after sweeping away the unreacted precursors and byproducts. This can be considered as a surface grafting process taking place in the gas phase. Mondloch et al. [154] used this semi-ALD process to modify MOFs. There were three prerequisites for the MOFs to be modified by semi-ALD, i.e. the proper pore size, good thermal stability, and accessible functional groups. They synthesized a Zr-based MOF (NU-1000) as substrates. The NU-1000 was composed of micropores (~12 Å) and mesopores (30 Å). This MOF material is stable at 500°C and possesses hydroxyl groups in the pores for further ALD modification. They demonstrated that 120 s exposure time of the precursor, DEZ or TMA, were enough for three Zn or eight Al atoms combining with Zr_6 node (Fig. 14b), while the solution-based method required several hours to achieve the same result. This semi-ALD process metallized NU-1000, and reduced its pore size from ~30 Å to ~27 Å, implying its great capability to tune pores in the level of angstrom. Brožová et al. [155] used the semi-ALD process to introduce (−)-α-pinene into Al_2O_3-deposited PC membranes. Thus-modified membranes exhibited significantly increased sorption towards single (−)-α-pinene rather than the (+)-α-pinene and racemate, enabling chiral molecule separation. Clearly, semi-ALD is able to tune the pore size and modify the pore chemistry of membranes. As semi-ALD involves only one single exposure to the precursor to build molecular monolayers on the surface of fine pores, it is more suitable for the tuning of pore sizes of NF and gas-separation membranes with micropores as grafting of monolayers of molecules is adequate to significantly reduce the pore sizes. More works are going to appear in this specific area as semi-ALD has rarely been used to modify/functionalize membranes although it has great potential in this regard.

In an early application related to gas separation, ALD was used to deposit Al_2O_3 on high-density polyethylene (HDPE) particles, then the modified particles were extruding to form films [156]. During the extruding processes, the uniform Al_2O_3 deposition layers were broken into flakes and doped into the polymeric films. For the HDPE particles with an average diameter of 60 μm, the diffusion coefficient and permeability of the polymer films towards He gas were reduced by ~15%. However, the diffusion coefficient was reduced by only 7.3% and the permeability were increased by ~100% for the films fabricated from smaller HDPE particles (16 μm). This result was ascribed to the voids between the Al_2O_3 flakes and polymers. After modified by the silane agents before extruding processes, the films fabricated from smaller particles showed a ~20% decrement of both the diffusion coefficient and the permeability. By choosing certain ALD processes and polymer particles, the size and thickness of doped inorganics can be precisely controlled. This work suggests an effective way to prepare mixed-matrix membranes, which perfectly overcomes the long-standing challenge of homogeneously dispersing inorganic fillers into the polymer matrix.

Typically, ALD modification takes place on both sides of membranes, producing membranes with identical coatings on each side. However, an interesting ALD process for the preparation of Janus membranes has been reported. By sealing one side of PP membranes, the deposition of hydrophilic Al_2O_3 was successfully restricted on the other side of PP membranes, thus producing hydrophilic (Al_2O_3)-hydrophobic (PP) Janus membranes [157]. For hydrophilic membranes, the gas had to exhaust the liquid in membrane pores at aeration processes. For hydrophobic membranes, the gas bubbles were hard to get off the membrane surface. Therefore, a membrane with hydrophilic surface and hydrophobic pore walls was particularly suitable for aeration processes. The hydrophilic surface minimized the adhesion between gas bubbles and PP membranes, which would greatly reduce the energy consumption in the aeration processes.

10. Conclusions and perspectives

In this review, we discuss the mechanism, chemistry and process of ALD in the context of membrane separation, analyze the merits of ALD in the modification and functionalization of membranes, and summarize recent progresses in the applications of ALD upgrading membrane performance and in the providing new functions to membranes. As an advanced gas-phase deposition process, ALD can deposit metals, oxides, polymers and many other materials on both polymeric and inorganic membranes. Compared to other deposition techniques, ALD is distinguished for its strong capability to conformally coat wall surfaces of pores with sizes down to the molecular level. Consequently, membrane pores can be tailored both in surface chemistry and pore sizes by ALD, enabling the controllable transformation of wettability and fine tuning of pore diameters with the precision at the angstrom level. After ALD treatment, membranes can obtain direct performance improvement or serve as intermediates for additional functionalization. Most strikingly, ALD is able to break the frustrating trade-off effect in membrane separation, that is, simultaneously improve the permeability and selectivity of the membranes, because ALD of metal oxides strongly enhances the hydrophilicity of polymeric membranes at the cost of slight decrease in pore size. In the direct performance improvement, some important properties of membranes, including selectivity, permeability, fouling resistance, wettability, mechanical robustness, thermal and chemical stabilities, are enhanced to various extents. In the indirect applications, the ALD-deposited materials can work as metal sources, functional layers, seeding layers or transition layers to prepare separation membranes with additional functions such as catalysis, photocatalysis, adsorption, and antibacterial activity.

Although ALD has many advantages and huge potentials as we discussed above, the costly precursors, complicated operating procedures, and slow growth rate restrict its large-scale utilization in membrane separation which is far more cost-sensitive than microelectronics. There are some fundamental and technical challenges regarding to ALD precursors, processes, and devices remained to be solved. Due to the high cost and excessive dosage at pulse steps, the large consumption of precursors may be a heavy burden. Comparing with the high-added-value microelectronic industries, the membrane industries may be unlikely to bear the costly precursor consumption. Therefore, it is necessary to source or synthesize cheaper substitutes. Moreover, ultrahigh purity of the precursors required for the ALD applications in microelectronics is not necessary in its usages for membranes, which would greatly reduce the precursor costs. In addition, excessive precursors are pulsed into the reaction chamber and wasted in the purge steps. Extraction units can be added between the chamber and the vacuum pump, which will recover the precursors from the purge gas and reduce the consumption. The

commonly used membranes including NF and RO membranes are prepared from solution-based processes such as phase inversion and interfacial polymerization, and they are "wet" membranes. Their surfaces are hydrated with water and their pores are filled with water. Consequently, these wet membranes cannot be directly subjected to ALD treatment as the high vacuum and elevated temperature may destroy their vulnerable porous structures, and water in the membranes will significantly intervene the ALD process. Atmospheric ALD requiring no vacuum would be an important solution to this annoying challenge, and more efforts should be made to optimize this special ALD process towards the specific requirements of membranes.

ALD devices are another main obstacle for the real-world applications of ALD in the membrane field. Typical ALD devices have flat reaction chambers with relatively small sizes as they are originally designed for the processing of silicon wafers in the shape of thin plates. However, industrialized membranes are usually present in the form of rolls of continuous films or bundles of long fibers, and are used as modules with the length typically larger than 1 m and the diameter of several tens of centimeters. For the sake of productivity, membranes should be treated in the ALD chamber in large volumes or in the entire membrane modules, requiring correspondingly large-sized ALD chambers. Significant works should be done to design such big chambers and to re-design the entire ALD system including the device and the deposition process. Alternatively, roll-to-roll ALD devices are expected to continuously treat membranes in the form of flat sheets with high productivity.

The ALD-deposited membranes themselves deserve extensive investigations as they are a new type of composite materials of layered structures with interlaced interfaces. A main point is the compatibility between the deposition layer and the membrane substrates. The difference in physical and chemical properties such as mechanical strength, chemical stability, thermal expansion and stability of them may weaken the long-term performance of the deposited membranes. For example, the metal oxides deposited on polymeric membranes can significantly improve the separation performance, while the rigid metal oxides may reduce the elasticity of polymeric membranes. Additionally, the polymer deposited on the ceramic membranes may not tolerate harsh operating conditions.

Although significant advances have been achieved in the applications of ALD in the membrane field, we believe the potentials of ALD to upgrade membranes have not been fully explored, and there are more chances for membranes to take further use of ALD. At least, the following topics summarized below are worthwhile of immediate actions. Up to date, ALD has been exclusively use to deposit single-component materials on membranes. By changing ALD deposition sequences, the "A-B" deposition mode can be easily turned into "A-B-C" mode. This would enable the deposition of hybrid materials on substrate membranes, producing membranes with better performance or multiple functions. Innovation in the deposition process may bring new opportunities to tune the microstructure of the membranes, thus enhancing the membrane performances. A direct example is to establish an asymmetric porosity in substrate membranes by optimizing the deposition parameters, which may significantly improve rejection at slight expense of permeation. More materials with intrinsic porosity such as framework materials and conjugated microporous polymers are expected to be synthesized by ALD after careful design of precursors and process development. If they are synthesized on the surfaces of porous substrates, advanced membranes with fast permeation and tight rejection will be obtained.

Originally designed for microelectronics, ALD is not widely known in the membrane community, and its potential in membrane functionalization and synthesis of new membranes is far from adequately explored. ALD has not yet been used in industry to treat separation membranes. However, we anticipate that the large-scale application of ALD may first appear in the treatment of "dry" membranes such as inorganic membranes (ceramic, zeolite, etc.), polymeric MF membranes having large pores, polyolefin membranes prepared by the stretching process as they require least care in the ALD treatment. We expect this review to attract more attentions from membrane insiders to ALD on one hand, and also to call for interests among researchers and engineers working in precursor synthesis, process development, and equipment design of ALD to the needs of the membrane community on the other. With continuous efforts from both sides, ALD will become a pervasive industrial technique for membrane modification/functionalization, and next-generation membranes with precise structure and on-demand functions will be available by taking full advantage of ALD.

CRediT authorship contribution statement

Sen Xiong: Investigation, Data curation, Writing – original draft, Writing – review & editing. **Xiaofeng Qian:** Investigation, Writing – review & editing, Validation. **Zhaoxiang Zhong:** Writing – review & editing, Validation. **Yong Wang:** Conceptualization, Writing – review & editing, Supervision, All authors have approved to the final version of the manuscript.

Declaration of competing interest

The authors declare that they have no known competing financial interests or personal relationships that could have appeared to influence the work reported in this paper.

Data availability

No data was used for the research described in the article.

Acknowledgements

Financial supports from the National Natural Science Foundation of China (21908096, 21825803), the Jiangsu Natural Science Foundation (BK20190677), and the National Basic Research Program of China (2015CB655301) are acknowledged. Y. W. thanks the former group members who have participated in the studies of upgrading membrane performance by atomic layer deposition since 2009.

References

[1] D.S. Sholl, R.P. Lively, Seven chemical separations to change the world, Nature 532 (2016) 435.
[2] D. Li, Y. Yan, H. Wang, Recent advances in polymer and polymer composite membranes for reverse and forward osmosis processes, Prog. Polym. Sci. 61 (2016) 104–155.
[3] D.S. Sholl, R.P. Lively, Seven chemical separations to change the world, Nature 532 (2016) 435–437.
[4] F. Galiano, K. Briceño, T. Marino, A. Molino, K.V. Christensen, A. Figoli, Advances in biopolymer-based membrane preparation and applications, J. Membr. Sci. 564 (2018) 562–586.
[5] H. Strathmann, K. Kock, P. Amar, R.W. Baker, The formation mechanism of asymmetric membranes, Desalination 16 (1975) 179–203.
[6] G.-d. Kang, Y.-m. Cao, Application and modification of poly(vinylidene fluoride) (PVDF) membranes – a review, J. Membr. Sci. 463 (2014) 145–165.
[7] R. Zhang, Y. Liu, M. He, Y. Su, X. Zhao, M. Elimelech, Z. Jiang, Antifouling membranes for sustainable water purification: strategies and mechanisms, Chem. Soc. Rev. 45 (2016) 5888–5924.
[8] X. Zhang, J. Tian, S. Gao, Z. Zhang, F. Cui, C.Y. Tang, In situ surface modification of thin film composite forward osmosis membranes with sulfonated poly(arylene ether sulfone) for anti-fouling in emulsified oil/water separation, J. Membr. Sci. 527 (2017) 26–34.
[9] L. Shen, S. Feng, J. Li, J. Chen, F. Li, H. Lin, G. Yu, Surface modification of polyvinylidene fluoride (PVDF) membrane via radiation grafting: novel mechanisms underlying the interesting enhanced membrane performance, Sci. Rep. 7 (2017) 2721.
[10] Y. Chul Woo, Y. Chen, L.D. Tijing, S. Phuntsho, T. He, J.-S. Choi, S.-H. Kim, H. Kyong Shon, CF_4 plasma-modified omniphobic electrospun nanofiber membrane for produced water brine treatment by membrane distillation, J. Membr. Sci. 529 (2017) 234–242.
[11] M. Safarpour, V. Vatanpour, A. Khataee, H. Zarrabi, P. Gholami, M. E. Yekavalangi, High flux and fouling resistant reverse osmosis membrane modified with plasma treated natural zeolite, Desalination 411 (2017) 89–100.

[12] F. Zareei Pour, M.M. Sabzehmeidani, H. Karimi, V. Madadi Avargani, M. Ghaedi, Superhydrophobic–superoleophilic electrospun nanofibrous membrane modified by the chemical vapor deposition of dimethyl dichlorosilane for efficient oil–water separation, J. Appl. Polym. Sci. 136 (2019), 47621.

[13] M. Nomura, T. Yamaguchi, S.-i. Nakao, Silicalite membranes modified by counterdiffusion CVD technique, Ind. Eng. Chem. Res. 36 (1997) 4217–4223.

[14] A.I. Pereira, P. Pérez, S.C. Rodrigues, A. Mendes, L.M. Madeira, C.J. Tavares, Deposition of Pd–Ag thin film membranes on ceramic supports for hydrogen purification/separation, Mater. Res. Bull. 61 (2015) 528–533.

[15] T.P. Martin, K.K.S. Lau, K. Chan, Y. Mao, M. Gupta, W. Shannan O'Shaughnessy, K.K. Gleason, Initiated chemical vapor deposition (iCVD) of polymeric nanocoatings, Surf. Coating. Technol. 201 (2007) 9400–9405.

[16] M. Leskelä, M. Ritala, Atomic layer deposition (ALD): from precursors to thin film structures, Thin Solid Films 409 (2002) 138–146.

[17] R.L. Puurunen, A short history of atomic layer deposition: Tuomo Suntola's atomic layer epitaxy, Chem. Vap. Depos. 20 (2014) 332–344.

[18] G. Song, D.Q. Tan, Atomic layer deposition for polypropylene film engineering—a review, Macromol. Mater. Eng. 305 (2020), 2000127.

[19] R.W. Johnson, A. Hultqvist, S.F. Bent, A brief review of atomic layer deposition: from fundamentals to applications, Mater, Today Off. 17 (2014) 236–246.

[20] G.N. Parsons, J.W. Elam, S.M. George, S. Haukka, H. Jeon, W.M.M. Kessels, M. Leskelä, P. Poodt, M. Ritala, S.M. Rossnagel, History of atomic layer deposition and its relationship with the American Vacuum Society, J. Vac. Sci. Technol., A 31 (2013), 050818.

[21] Y. Zhao, L. Zhang, J. Liu, K. Adair, F. Zhao, Y. Sun, T. Wu, X. Bi, K. Amine, J. Lu, X. Sun, Atomic/molecular layer deposition for energy storage and conversion, Chem. Soc. Rev. 50 (2021) 3889–3956.

[22] Y. Zhao, K. Zheng, X. Sun, Addressing interfacial issues in liquid-based and solid-state batteries by atomic and molecular layer deposition, Joule 2 (2018) 2583–2604.

[23] P.O. Oviroh, R. Akbarzadeh, D. Pan, R.A.M. Coetzee, T.-C. Jen, New development of atomic layer deposition: processes, methods and applications, Sci. Technol. Adv. Mater. 20 (2019) 465–496.

[24] C. Marichy, M. Bechelany, N. Pinna, Atomic layer deposition of nanostructured materials for energy and environmental applications, Adv. Mater. 24 (2012) 1017–1032.

[25] B.J. O'Neill, D.H.K. Jackson, J. Lee, C. Canlas, P.C. Stair, C.L. Marshall, J. W. Elam, T.F. Kuech, J.A. Dumesic, G.W. Huber, Catalyst design with atomic layer deposition, ACS Catal. 5 (2015) 1804–1825.

[26] G.N. Parsons, S.E. Atanasov, E.C. Dandley, C.K. Devine, B. Gong, J.S. Jur, K. Lee, C.J. Oldham, Q. Peng, J.C. Spagnola, P.S. Williams, Mechanisms and reactions during atomic layer deposition on polymers, Coord. Chem. Rev. 257 (2013) 3323–3331.

[27] S.J. Lim, S.-j. Kwon, H. Kim, J.-S. Park, High performance thin film transistor with low temperature atomic layer deposition nitrogen-doped ZnO, Appl. Phys. Lett. 91 (2007), 183517.

[28] E. Guziewicz, I.A. Kowalik, M. Godlewski, K. Kopalko, V. Osinniy, A. Wójcik, S. Yatsunenko, E. Łusakowska, W. Paszkowicz, M. Guziewicz, Extremely low temperature growth of ZnO by atomic layer deposition, J. Appl. Phys. 103 (2008), 033515.

[29] M.J. Biercuk, D.J. Monsma, C.M. Marcus, J.S. Becker, R.G. Gordon, Low-temperature atomic-layer-deposition lift-off method for microelectronic and nanoelectronic applications, Appl. Phys. Lett. 83 (2003) 2405–2407.

[30] J. Meyer, D. Schneidenbach, T. Winkler, S. Hamwi, T. Weimann, P. Hinze, S. Ammermann, H.-H. Johannes, T. Riedl, W. Kowalsky, Reliable thin film encapsulation for organic light emitting diodes grown by low-temperature atomic layer deposition, Appl. Phys. Lett. 94 (2009), 233305.

[31] S. Kim, G.R. Gavalas, Preparation of H_2 permselective silica membranes by alternating reactant vapor deposition, Ind. Eng. Chem. Res. 34 (1995) 168–176.

[32] G. Triani, P.J. Evans, D.J. Attard, K.E. Prince, J. Bartlett, S. Tan, R.P. Burford, Nanostructured TiO_2 membranes by atomic layer deposition, J. Mater. Chem. 16 (2006) 1355–1359.

[33] F. Li, L. Li, X. Liao, Y. Wang, Precise pore size tuning and surface modifications of polymeric membranes using the atomic layer deposition technique, J. Membr. Sci. 385–386 (2011) 1–9.

[34] M. Weber, A. Julbe, A. Ayral, P. Miele, M. Bechelany, Atomic layer deposition for membranes: basics, challenges, and opportunities, Chem. Mater. 30 (2018) 7368–7390.

[35] B.A. McCool, W.J. DeSisto, Synthesis and characterization of silica membranes prepared by pyridine-catalyzed atomic layer deposition, Ind. Eng. Chem. Res. 43 (2004) 2478–2484.

[36] B.A. McCool, W.J. DeSisto, Amino-functionalized silica membranes for enhanced carbon dioxide permeation, Adv. Funct. Mater. 15 (2005) 1635–1640.

[37] L. Velleman, G. Triani, P.J. Evans, J.G. Shapter, D. Losic, Structural and chemical modification of porous alumina membranes, Microporous Mesoporous Mater. 126 (2009) 87–94.

[38] X. Liang, X. Lu, M. Yu, A.S. Cavanagh, D.L. Gin, A.W. Weimer, Modification of nanoporous supported lyotropic liquid crystal polymer membranes by atomic layer deposition, J. Membr. Sci. 349 (2010) 1–5.

[39] H.-C. Yang, R.Z. Waldman, Z. Chen, S.B. Darling, Atomic layer deposition for membrane interface engineering, Nanoscale 10 (2018) 20505–20513.

[40] M. Weber, A. Julbe, S.S. Kim, M. Bechelany, Atomic layer deposition (ALD) on inorganic or polymeric membranes, J. Appl. Phys. 126 (2019), 041101.

[41] H. Van Bui, F. Grillo, J.R. van Ommen, Atomic and molecular layer deposition: off the beaten track, Chem. Commun. 53 (2017) 45–71.

[42] Q. Xu, Y. Yang, X. Wang, Z. Wang, W. Jin, J. Huang, Y. Wang, Atomic layer deposition of alumina on porous polytetrafluoroethylene membranes for enhanced hydrophilicity and separation performances, J. Membr. Sci. 415–416 (2012) 435–443.

[43] Q. Wang, X. Wang, Z. Wang, J. Huang, Y. Wang, PVDF membranes with simultaneously enhanced permeability and selectivity by breaking the tradeoff effect via atomic layer deposition of TiO_2, J. Membr. Sci. 442 (2013) 57–64.

[44] X. Jia, Z. Low, H. Chen, S. Xiong, Y. Wang, Atomic layer deposition of Al_2O_3 on porous polypropylene hollow fibers for enhanced membrane performances, Chin. J. Chem. Eng. 26 (2018) 695–700.

[45] S. Xiong, X. Jia, K. Mi, Y. Wang, Upgrading polytetrafluoroethylene hollow-fiber membranes by CFD-optimized atomic layer deposition, J. Membr. Sci. 617 (2021), 118610.

[46] N. Li, Y. Tian, J. Zhao, J. Zhang, L. Kong, J. Zhang, W. Zuo, Static adsorption of protein-polysaccharide hybrids on hydrophilic modified membranes based on atomic layer deposition: anti-fouling performance and mechanism insight, J. Membr. Sci. 548 (2018) 470–480.

[47] T. Sheng, H. Chen, S. Xiong, X. Chen, Y. Wang, Atomic layer deposition of polyimide on microporous polyethersulfone membranes for enhanced and tunable performances, AIChE J. 60 (2014) 3614–3622.

[48] N. Li, Y. Tian, J. Zhang, Z. Sun, J. Zhao, J. Zhang, W. Zuo, Precisely-controlled modification of PVDF membranes with 3D TiO_2/ZnO nanolayer: enhanced anti-fouling performance by changing hydrophilicity and photocatalysis under visible light irradiation, J. Membr. Sci. 528 (2017) 359–368.

[49] W. Yang, M. Son, R. Rossi, J.S. Vrouwenvelder, B.E. Logan, Adapting aluminum-doped zinc oxide for electrically conductive membranes fabricated by atomic layer deposition, ACS Appl. Mater. Interfaces 12 (2020) 963–969.

[50] S. Xiong, L. Kong, Z.X. Zhong, Y. Wang, Dye adsorption on zinc oxide nanoparticulates atomic-layer-deposited on polytetrafluoroethylene membranes, AIChE J. 62 (2016) 3982–3991.

[51] H.-C. Yang, Y. Xie, H. Chan, B. Narayanan, L. Chen, R.Z. Waldman, S.K.R. S. Sankaranarayanan, J.W. Elam, S.B. Darling, Crude-oil-repellent membranes by atomic layer deposition: oxide interface engineering, ACS Nano 12 (2018) 8678–8685.

[52] S. Chaudhury, E. Wormser, Y. Harari, E. Edri, O. Nir, Tuning the ion-selectivity of thin-film composite nanofiltration membranes by molecular layer deposition of alucone, ACS Appl. Mater. Interfaces 12 (2020) 53356–53364.

[53] Z. Song, M. Fathizadeh, Y. Huang, K.H. Chu, Y. Yoon, L. Wang, W.L. Xu, M. Yu, TiO_2 nanofiltration membranes prepared by molecular layer deposition for water purification, J. Membr. Sci. 510 (2016) 72–78.

[54] H. Chen, X. Jia, M. Wei, Y. Wang, Ceramic tubular nanofiltration membranes with tunable performances by atomic layer deposition and calcination, J. Membr. Sci. 528 (2017) 95–102.

[55] M. Drobek, M. Bechelany, C. Vallicari, A. Abou Chaaya, C. Charmette, C. Salvador-Levehang, P. Miele, A. Julbe, An innovative approach for the preparation of confined ZIF-8 membranes by conversion of ZnO ALD layers, J. Membr. Sci. 475 (2015) 39–46.

[56] X. Ma, P. Kumar, N. Mittal, A. Khlyustova, P. Daoutidis, K.A. Mkhoyan, M. Tsapatsis, Zeolitic imidazolate framework membranes made by ligand-induced permselectivation, Science 361 (2018) 1008–1011.

[57] T.-N. Kim, J. Lee, J.-H. Choi, J.-H. Ahn, E. Yang, M.-H. Hwang, K.-J. Chae, Tunable atomic level surface functionalization of a multi-layered graphene oxide membrane to break the permeability-selectivity trade-off in salt removal of brackish water, Separ. Purif. Technol. 274 (2021), 119047.

[58] Q. Xu, J. Yang, J. Dai, Y. Yang, X. Chen, Y. Wang, Hydrophilization of porous polypropylene membranes by atomic layer deposition of TiO_2 for simultaneously improved permeability and selectivity, J. Membr. Sci. 448 (2013) 215–222.

[59] Q. Xu, Y. Yang, J. Yang, X. Wang, Z. Wang, Y. Wang, Plasma activation of porous polytetrafluoroethylene membranes for superior hydrophilicity and separation performances via atomic layer deposition of TiO_2, J. Membr. Sci. 443 (2013) 62–68.

[60] H. Chen, L. Kong, Y. Wang, Enhancing the hydrophilicity and water permeability of polypropylene membranes by nitric acid activation and metal oxide deposition, J. Membr. Sci. 487 (2015) 109–116.

[61] N. Li, J. Zhang, Y. Tian, J. Zhang, W. Zhan, J. Zhao, Y. Ding, W. Zuo, Hydrophilic modification of polyvinylidene fluoride membranes by ZnO atomic layer deposition using nitrogen dioxide/diethylzinc functionalization, J. Membr. Sci. 514 (2016) 241–249.

[62] J. Alam, M. Alhoshan, L.A. Dass, A.K. Shukla, M.R. Muthumareeswaran, M. Hussain, A.S. Aldwayyan, Atomic layer deposition of TiO_2 film on a polyethersulfone membrane: separation applications, J. Polym. Res. 23 (2016) 183.

[63] N. Li, J. Zhang, Y. Tian, J. Zhao, J. Zhang, W. Zuo, Anti-fouling potential evaluation of PVDF membranes modified with ZnO against polysaccharide, Chem. Eng. J. 304 (2016) 165–174.

[64] S.-M. Lee, V. Ischenko, E. Pippel, A. Masic, O. Moutanabbir, P. Fratzl, M. Knez, An alternative route towards metal–polymer hybrid materials prepared by vapor-phase processing, Adv. Funct. Mater. 21 (2011) 3047–3055.

[65] F. Kayaci, C. Ozgit-Akgun, N. Biyikli, T. Uyar, Surface-decorated ZnO nanoparticles and ZnO nanocoating on electrospun polymeric nanofibers by atomic layer deposition for flexible photocatalytic nanofibrous membranes, RSC Adv. 3 (2013) 6817–6820.

[66] C. Li, L.P. Ren, X. Liu, C.H. Zhang, D.Z. Chen, W.L. Xu, Y. Qin, Superhydrophilic and underwater superoleophobic poly(propylene) nonwoven coated with TiO_2 by atomic layer deposition, Adv. Mater. Interfac. 8 (2021).

[67] J. Lu, Y. Li, W. Song, M.D. Losego, R. Monikandan, K.I. Jacob, R. Xiao, Atomic layer deposition onto thermoplastic polymeric nanofibrous aerogel templates for tailored surface properties, ACS Nano 14 (2020) 7999–8011.

[68] Y. Li, L. Chen, J.P. Wooding, F. Zhang, R.P. Lively, R. Ramprasad, M.D. Losego, Controlling wettability, wet strength, and fluid transport selectivity of nanopaper with atomic layer deposited (ALD) sub-nanometer metal oxide coatings, Nanoscale Adv. 2 (2020) 356–367.

[69] J. Nikkola, J. Sievänen, M. Raulio, J. Wei, J. Vuorinen, C.Y. Tang, Surface modification of thin film composite polyamide membrane using atomic layer deposition method, J. Membr. Sci. 450 (2014) 174–180.

[70] X. Zhou, Y.-Y. Zhao, S.-R. Kim, M. Elimelech, S. Hu, J.-H. Kim, Controlled TiO_2 growth on reverse osmosis and nanofiltration membranes by atomic layer deposition: mechanisms and potential applications, Environ. Sci. Technol. 52 (2018) 14311–14320.

[71] P. Juholin, M.-L. Kääriäinen, M. Riihimäki, R. Sliz, J.L. Aguirre, M. Pirilä, T. Fabritius, D. Cameron, R.L. Keiski, Comparison of ALD coated nanofiltration membranes to unmodified commercial membranes in mine wastewater treatment, Separ. Purif. Technol. 192 (2018) 69–77.

[72] K. Zarshenas, G. Jiang, J. Zhang, M.A. Jauhar, Z. Chen, Atomic scale manipulation of sublayer with functional TiO_2 nanofilm toward high-performance reverse osmosis membrane, Desalination 480 (2020), 114342.

[73] H. Chen, Q. Lin, Q. Xu, Y. Yang, Z. Shao, Y. Wang, Plasma activation and atomic layer deposition of TiO_2 on polypropylene membranes for improved performances of lithium-ion batteries, J. Membr. Sci. 458 (2014) 217–224.

[74] A. DeStefano, J. Yin, T.J. Kraus, B.A. Parkinson, K.D. Li-Oakey, Elucidation of titanium dioxide nucleation and growth on a polydopamine-modified nanoporous polyvinylidene fluoride substrate via low-temperature atomic layer deposition, ACS Omega 3 (2018) 10493–10502.

[75] X. Yang, P. Sun, H. Zhang, Z. Xia, R.Z. Waldman, A.U. Mane, J.W. Elam, L. Shao, S.B. Darling, Polyphenol-sensitized atomic layer deposition for membrane interface hydrophilization, Adv. Funct. Mater. 30 (2020), 1910062.

[76] Y. Guo, J. Chen, X. Hao, J. Zhang, X. Feng, H. Zhang, A novel process for preparing expanded Polytetrafluoroethylene(ePTFE) micro-porous membrane through ePTFE/ePTFE co-stretching technique, J. Mater. Sci. 42 (2007) 2081–2085.

[77] Z. Zhong, Z. Xu, T. Sheng, J. Yao, W. Xing, Y. Wang, Unusual air filters with ultrahigh efficiency and antibacterial functionality enabled by zno nanorods, ACS Appl. Mater. Interfaces 7 (2015) 21538–21544.

[78] S. Feng, D. Li, Z.-x. Low, Z. Liu, Z. Zhong, Y. Hu, Y. Wang, W. Xing, ALD-seeded hydrothermally-grown Ag/ZnO nanorod PTFE membrane as efficient indoor air filter, J. Membr. Sci. 531 (2017) 86–93.

[79] L. Zhang, X. Shi, M. Sun, C.J. Porter, X. Zhou, M. Elimelech, Precisely engineered photoreactive titanium nanoarray coating to mitigate biofouling in ultrafiltration, ACS Appl. Mater. Interfaces 13 (2021) 9975–9984.

[80] L. Kong, Q. Wang, S. Xiong, Y. Wang, Turning low-cost filter papers to highly efficient membranes for oil/water separation by atomic-layer-deposition-enabled hydrophobization, Ind. Eng. Chem. Res. 53 (2014) 16516–16522.

[81] S. Xiong, L. Kong, J. Huang, X. Chen, Y. Wang, Atomic-layer-deposition-enabled nonwoven membranes with hierarchical ZnO nanostructures for switchable water/oil separations, J. Membr. Sci. 493 (2015) 478–485.

[82] A. Huang, C.-C. Kan, S.-C. Lo, L.-H. Chen, D.-Y. Su, J.F. Soesanto, C.-C. Hsu, F.-Y. Tsai, K.-L. Tung, Nanoarchitectured design of porous ZnO@copper membranes enabled by atomic-layer-deposition for oil/water separation, J. Membr. Sci. 582 (2019) 120–131.

[83] R. Huang, Z. Liu, Y.C. Woo, W. Luo, S.R. Gray, M. Xie, Emerging investigator series: engineering membrane distillation with nanofabrication: design, performance and mechanisms, Environ. Sci. J. Integr. Environ. Res.: Water Research & Technology 6 (2020) 1786–1793.

[84] A.I. Abdulagatov, K.E. Terauds, J.J. Travis, A.S. Cavanagh, R. Raj, S.M. George, Pyrolysis of titanicone molecular layer deposition films as precursors for conducting TiO_2/carbon composite films, J. Phys. Chem. C 117 (2013) 17442–17450.

[85] A.I. Abdulagatov, R.A. Hall, J.L. Sutherland, B.H. Lee, A.S. Cavanagh, S. M. George, Molecular layer deposition of titanicone films using $TiCl_4$ and ethylene glycol or glycerol: growth and properties, Chem. Mater. 24 (2012) 2854–2863.

[86] F. Li, Y. Yang, Y. Fan, W. Xing, Y. Wang, Modification of ceramic membranes for pore structure tailoring: the atomic layer deposition route, J. Membr. Sci. 397–398 (2012) 17–23.

[87] H. Chen, S. Wu, X. Jia, S. Xiong, Y. Wang, Atomic layer deposition fabricating of ceramic nanofiltration membranes for efficient separation of dyes from water, AIChE J. 64 (2018) 2670–2678.

[88] S. Wu, Z. Wang, S. Xiong, Y. Wang, Tailoring TiO_2 membranes for nanofiltration and tight ultrafiltration by leveraging molecular layer deposition and crystallization, J. Membr. Sci. 578 (2019) 149–155.

[89] K.-H. Park, P.-F. Sun, E.H. Kang, G.D. Han, B.J. Kim, Y. Jang, S.-H. Lee, J.H. Shim, H.-D. Park, Photocatalytic anti-biofouling performance of nanoporous ceramic membranes treated by atomic layer deposited ZnO, Separ. Purif. Technol. 272 (2021), 118935.

[90] H. Zhang, A.U. Mane, X. Yang, Z. Xia, E.F. Barry, J. Luo, Y. Wan, J.W. Elam, S. B. Darling, Visible-light-activated photocatalytic films toward self-cleaning membranes, Adv. Funct. Mater. 30 (2020), 2002847.

[91] A. Lee, J.A. Libera, R.Z. Waldman, A. Ahmed, J.R. Avila, J.W. Elam, S.B. Darling, Conformal nitrogen-doped TiO_2 photocatalytic coatings for sunlight-activated membranes, Adv. Sustain. Syst. 1 (2017), 1600041.

[92] J. Lu, Q. Chen, S. Chen, H. Jiang, Y. Liu, R. Chen, Pd nanoparticles loaded on ceramic membranes by atomic layer deposition with enhanced catalytic properties, Ind. Eng. Chem. Res. 59 (2020) 19564–19573.

[93] T.H.Y. Tran, W.G. Haije, V. Longo, W.M.M. Kessels, J. Schoonman, Plasma-enhanced atomic layer deposition of titania on alumina for its potential use as a hydrogen-selective membrane, J. Membr. Sci. 378 (2011) 438–443.

[94] M. Weber, M. Drobek, B. Rebière, C. Charmette, J. Cartier, A. Julbe, M. Bechelany, Hydrogen selective palladium-alumina composite membranes prepared by atomic layer deposition, J. Membr. Sci. 596 (2020), 117701.

[95] R.J. Narayan, S.P. Adiga, M.J. Pellin, L.A. Curtiss, S. Stafslien, B. Chisholm, N. A. Monteiro-Riviere, R.L. Brigmon, J.W. Elam, Atomic layer deposition of nanoporous biomaterials, Mater. Today 13 (2010) 60–64.

[96] H.J. Lee, H.O. Seo, D.W. Kim, K.-D. Kim, Y. Luo, D.C. Lim, H. Ju, J.W. Kim, J. Lee, Y.D. Kim, A high-performing nanostructured TiO_2 filter for volatile organic compounds using atomic layer deposition, Chem. Commun. 47 (2011) 5605–5607.

[97] A. Vaish, S. Krueger, M. Dimitriou, C. Majkrzak, D.J. Vanderah, L. Chen, K. Gawrisch, Enhancing the platinum atomic layer deposition infiltration depth inside anodic alumina nanoporous membrane, J. Vac. Sci. Technol., A 33 (2015), 01A148.

[98] T. Yanagishita, M. Otsuka, T. Takei, S. Uto, H. Masuda, Preparation of ordered anodic porous alumina with single-nanometer-order-size holes by atomic layer deposition, Langmuir 37 (2021) 8331–8338.

[99] V. Vega, L. Gelde, A.S. González, V.M. Prida, B. Hernando, J. Benavente, Diffusive transport through surface functionalized nanoporous alumina membranes by atomic layer deposition of metal oxides, J. Ind. Eng. Chem. 52 (2017) 66–72.

[100] L. Gelde, A.L. Cuevas, J. Benavente, Influence of pore-size/porosity on ion transport and static BSA fouling for TiO_2-covered nanoporous alumina membranes, Appl. Sci. 11 (2021) 5687.

[101] I.-K. Oh, L. Zeng, J.-E. Kim, J.-S. Park, K. Kim, H. Lee, S. Seo, M.R. Khan, S. Kim, C.W. Park, J. Lee, B. Shong, Z. Lee, S.F. Bent, H. Kim, J.Y. Park, H.-B.-R. Lee, Surface energy change of atomic-scale metal oxide thin films by phase transformation, ACS Nano 14 (2020) 676–687.

[102] V. Romero, V. Vega, J. García, R. Zierold, K. Nielsch, V.M. Prida, B. Hernando, J. Benavente, Changes in morphology and ionic transport induced by ALD SiO_2 coating of nanoporous alumina membranes, ACS Appl. Mater. Interfaces 5 (2013) 3556–3564.

[103] A.L. Cuevas, M.V. Martínez de Yuso, L. Gelde, A.S. González, V. Vega, V.M. Prida, J. Benavente, Chemical, optical and transport characterization of ALD modified nanoporous alumina based structures, J. Ind. Eng. Chem. 91 (2020) 139–148.

[104] T.E. Berger, C. Regmi, A.I. Schäfer, B.S. Richards, Photocatalytic degradation of organic dye via atomic layer deposited TiO_2 on ceramic membranes in single-pass flow-through operation, J. Membr. Sci. 604 (2020), 118015.

[105] H.-S. Chen, P.-H. Chen, S.-H. Huang, T.-P. Perng, Toward highly efficient photocatalysis: a flow-through Pt@TiO_2@AAO membrane nanoreactor prepared by atomic layer deposition, Chem. Commun. 50 (2014) 4379–4382.

[106] H. Kang, Y. Sun, Y. Li, W. Qin, X. Wu, Mechanically robust fish-scale microstructured TiO_2-coated stainless steel mesh by atomic layer deposition for oil–water separation, Ind. Eng. Chem. Res. 59 (2020) 21088–21096.

[107] P. Zhang, J. Tong, Y. Jee, K. Huang, Stabilizing a high-temperature electrochemical silver-carbonate CO_2 capture membrane by atomic layer deposition of a ZrO_2 overcoat, Chem. Commun. 52 (2016) 9817–9820.

[108] L. Sainiemi, J. Viheriälä, T. Sikanen, J. Laukkanen, T. Niemi, Nanoperforated silicon membranes fabricated by UV-nanoimprint lithography, deep reactive ion etching and atomic layer deposition, J. Micromech. Microeng. 20 (2010), 077001.

[109] J. Feng, S. Xiong, Z. Wang, Z. Cui, S.-P. Sun, Y. Wang, Atomic layer deposition of metal oxides on carbon nanotube fabrics for robust, hydrophilic ultrafiltration membranes, J. Membr. Sci. 550 (2018) 246–253.

[110] J. Feng, S. Xiong, Y. Wang, Atomic layer deposition of TiO_2 on carbon-nanotube membranes for enhanced capacitive deionization, Separ. Purif. Technol. 213 (2019) 70–77.

[111] G. Zhang, D. Neagu, P.J. King, S. Ramadan, A. O'Neill, I.S. Metcalfe, The effects of sulphur poisoning on the microstructure, composition and oxygen transport properties of perovskite membranes coated with nanoscale alumina layers, J. Membr. Sci. 618 (2021), 118736.

[112] T. Sheng, L. Kong, Y. Wang, Crosslinking of polyimide atomic-layer-deposited on polyethersulfone membranes for synergistically enhanced performances, J. Membr. Sci. 486 (2015) 161–168.

[113] S. Xiong, T. Sheng, L. Kong, Z. Zhong, J. Huang, Y. Wang, Enhanced performances of polypropylene membranes by molecular layer deposition of polyimide, Chin. J. Chem. Eng. 24 (2016) 843–849.

[114] H. Wang, M. Wei, Z. Zhong, Y. Wang, Atomic-layer-deposition-enabled thin-film composite membranes of polyimide supported on nanoporous anodized alumina, J. Membr. Sci. 535 (2017) 56–62.

[115] B.C. Welch, O.M. McIntee, A.B. Ode, B.B. McKenzie, A.R. Greenberg, V.M. Bright, S.M. George, Continuous polymer films deposited on top of porous substrates using plasma-enhanced atomic layer deposition and molecular layer deposition, J. Vac. Sci. Technol., A 38 (2020), 052409.

[116] T. Yoshimura, S. Tatsuura, W. Sotoyama, A. Matsuura, T. Hayano, Quantum wire and dot formation by chemical vapor deposition and molecular layer deposition of one-dimensional conjugated polymer, Appl. Phys. Lett. 60 (1992) 268–270.

[117] S.E. Atanasov, M.D. Losego, B. Gong, E. Sachet, J.-P. Maria, P.S. Williams, G. N. Parsons, Highly conductive and conformal poly(3,4-ethylenedioxythiophene) (PEDOT) thin films via oxidative molecular layer deposition, Chem. Mater. 26 (2014) 3471–3478.

[118] A. Kim, M.A. Filler, S. Kim, S.F. Bent, Layer-by-Layer growth on Ge(100) via spontaneous urea coupling reactions, J. Am. Chem. Soc. 127 (2005) 6123–6132.
[119] T. Miyamae, K. Tsukagoshi, O. Matsuoka, S. Yamamoto, H. Nozoye, Preparation of polyimide-polyamide random copolymer thin film by sequential vapor deposition polymerization, Jpn. J. Appl. Phys. 41 (2002) 746–748.
[120] H. Li, M. Eddaoudi, M. O'Keeffe, O.M. Yaghi, Design and synthesis of an exceptionally stable and highly porous metal-organic framework, Nature 402 (1999) 276.
[121] H. Chen, A. Roy, J.-B. Baek, L. Zhu, J. Qu, L. Dai, Controlled growth and modification of vertically-aligned carbon nanotubes for multifunctional applications, Math. Sci. Eng. R 70 (2010) 63–91.
[122] S. Qiu, M. Xue, G. Zhu, Metal–organic framework membranes: from synthesis to separation application, Chem. Soc. Rev. 43 (2014) 6116–6140.
[123] D.-w. Choi, H. Park, J.H. Lim, T.H. Han, J.-S. Park, Three-dimensionally stacked Al_2O_3/graphene oxide for gas barrier applications, Carbon 125 (2017) 464–471.
[124] X. Chen, L. Wu, H. Yang, Y. Qin, X. Ma, N. Li, Tailoring the microporosity of polymers of intrinsic microporosity for advanced gas separation by atomic layer deposition 60 (2021) 17875–17880.
[125] K. Khaletskaya, S. Turner, M. Tu, S. Wannapaiboon, A. Schneemann, R. Meyer, A. Ludwig, G. Van Tendeloo, R.A. Fischer, Self-directed localization of ZIF-8 thin film formation by conversion of ZnO nanolayers, Adv. Funct. Mater. 24 (2014) 4804–4811.
[126] M. Bechelany, M. Drobek, C. Vallicari, A. Abou Chaaya, A. Julbe, P. Miele, Highly crystalline MOF-based materials grown on electrospun nanofibers, Nanoscale 7 (2015) 5794–5802.
[127] K.B. Lausund, V. Petrovic, O. Nilsen, All-gas-phase synthesis of amino-functionalized UiO-66 thin films, Dalton Trans. 46 (2017) 16983–16992.
[128] K.B. Lausund, M.S. Olsen, P.-A. Hansen, H. Valen, O. Nilsen, MOF thin films with bi-aromatic linkers grown by molecular layer deposition, J. Mater. Chem. 8 (2020) 2539–2548.
[129] M. Weber, B. Koonkaew, S. Balme, I. Utke, F. Picaud, I. Iatsunskyi, E. Coy, P. Miele, M. Bechelany, Boron nitride nanoporous membranes with high surface charge by atomic layer deposition, ACS Appl. Mater. Interfaces 9 (2017) 16669–16678.
[130] D. Naberezhnyi, L. Mai, N. Doudin, I. Ennen, A. Hütten, E.I. Altman, A. Devi, P. Dementyev, Molecular permeation in freestanding bilayer silica, Nano Lett. 22 (2022) 1287–1293.
[131] S.B.S. Heil, J.L.v. Hemmen, M.C.M.v.d. Sanden, W.M.M. Kessels, Reaction mechanisms during plasma-assisted atomic layer deposition of metal oxides: a case study for Al_2O_3, J. Appl. Phys. 103 (2008), 103302.
[132] P.M. Budd, B.S. Ghanem, S. Makhseed, N.B. McKeown, K.J. Msayib, C. E. Tattershall, Polymers of intrinsic microporosity (PIMs): robust, solution-processable, organic nanoporous materials, Chem. Commun. (2004) 230–231.
[133] I. Stassen, M. Styles, G. Grenci, Hans V. Gorp, W. Vanderlinden, Steven D. Feyter, P. Falcaro, D.D. Vos, P. Vereecken, R. Ameloot, Chemical vapour deposition of zeolitic imidazolate framework thin films, Nat. Mater. 15 (2015) 304.
[134] Z. Zhao, Y. Kong, X. Lin, C. Liu, J. Liu, Y. He, L. Yang, G. Huang, Y. Mei, Oxide nanomembrane induced assembly of a functional smart fiber composite with nanoporosity for an ultra-sensitive flexible glucose sensor, J. Mater. Chem. 8 (2020) 26119–26129.
[135] I. Pellejero, F. Almazán, M. Lafuente, M.A. Urbiztondo, M. Drobek, M. Bechelany, A. Julbe, L.M. Gandía, Functionalization of 3D printed ABS filters with MOF for toxic gas removal, J. Ind. Eng. Chem. 89 (2020) 194–203.
[136] Y. Lin, J.W. Connell, Advances in 2D boron nitride nanostructures: nanosheets, nanoribbons, nanomeshes, and hybrids with graphene, Nanoscale 4 (2012) 6908–6939.
[137] M.S. Driver, J.D. Beatty, O. Olanipekun, K. Reid, A. Rath, P.M. Voyles, J. A. Kelber, Atomic layer epitaxy of h-BN(0001) multilayers on Co(0001) and molecular beam epitaxy growth of Graphene on h-BN(0001)/Co(0001), Langmuir 32 (2016) 2601–2607.
[138] M. Snure, Q. Paduano, M. Hamilton, J. Shoaf, J.M. Mann, Optical characterization of nanocrystalline boron nitride thin films grown by atomic layer deposition, Thin Solid Films 571 (2014) 51–55.
[139] W. Hao, C. Marichy, C. Journet, A. Brioude, A novel two-step ammonia-free atomic layer deposition approach for boron nitride, ChemNanoMat 3 (2017) 656–663.
[140] P. Poodt, D.C. Cameron, E. Dickey, S.M. George, V. Kuznetsov, G.N. Parsons, F. Roozeboom, G. Sundaram, A. Vermeer, Spatial atomic layer deposition: a route towards further industrialization of atomic layer deposition, J. Vac. Sci. Technol., A 30 (2012), 010802.
[141] E. Dickey, W.A. Barrow, High rate roll to roll atomic layer deposition, and its application to moisture barriers on polymer films, J. Vac. Sci. Technol., A 30 (2012), 021502.
[142] K. Sharma, R.A. Hall, S.M. George, Spatial atomic layer deposition on flexible substrates using a modular rotating cylinder reactor, J. Vac. Sci. Technol., A 33 (2015), 01A132.
[143] P.R. Fitzpatrick, Z.M. Gibbs, S.M. George, Evaluating operating conditions for continuous atmospheric atomic layer deposition using a multiple slit gas source head, J. Vac. Sci. Technol., A 30 (2012), 01A136.
[144] J.-W. Lee, A.M. Soomro, M. Waqas, M.A.U. Khalid, K.H. Choi, A highly efficient surface modified separator fabricated with atmospheric atomic layer deposition for high temperature lithium ion batteries, Int. J. Energy Res. 44 (2020) 7035–7046.
[145] C.-H. Hsu, X.-P. Geng, W.-Y. Wu, M.-J. Zhao, X.-Y. Zhang, P.-H. Huang, S.-Y. Lien, Air annealing effect on oxygen vacancy defects in Al-doped ZnO films grown by high-speed atmospheric atomic layer deposition, Molecules 25 (2020) 5043.
[146] T. Van Gestel, H. Kruidhof, D.H.A. Blank, H.J.M. Bouwmeester, ZrO_2 and TiO_2 membranes for nanofiltration and pervaporation: Part 1. Preparation and characterization of a corrosion-resistant ZrO_2 nanofiltration membrane with a MWCO<300, J. Membr. Sci. 284 (2006) 128–136.
[147] R. Shang, A. Goulas, C.Y. Tang, X. de Frias Serra, L.C. Rietveld, S.G.J. Heijman, Atmospheric pressure atomic layer deposition for tight ceramic nanofiltration membranes: synthesis and application in water purification, J. Membr. Sci. 528 (2017) 163–170.
[148] K.-I. Liu, C.-C. Kei, M. Mishra, P.-H. Chen, W.-S. Liu, T.-P. Perng, Uniform coating of TiO_2 on high aspect ratio substrates with complex morphology by vertical forced-flow atomic layer deposition, RSC Adv. 7 (2017) 34730–34735.
[149] M. Mishra, C.-Y. Chan, C.-C. Kei, Y.-C. Yen, M.-W. Liao, T.-P. Perng, Forced flow atomic layer deposition of TiO_2 on vertically aligned Si wafer and polysulfone fiber: design and efficacy of conduit plates and soak function, Rev. Sci. Instrum. 89 (2018), 105108.
[150] Q. Peng, Y.-C. Tseng, S.B. Darling, J.W. Elam, A route to nanoscopic materials via sequential infiltration synthesis on block copolymer templates, ACS Nano 5 (2011) 4600–4606.
[151] D. Berman, S. Guha, B. Lee, J.W. Elam, S.B. Darling, E.V. Shevchenko, Sequential infiltration synthesis for the design of low refractive index surface coatings with controllable thickness, ACS Nano 11 (2017) 2521–2530.
[152] R.Z. Waldman, D. Choudhury, D.J. Mandia, J.W. Elam, P.F. Nealey, A.B. F. Martinson, S.B. Darling, Sequential infiltration synthesis of Al_2O_3 in polyethersulfone membranes, JOM 71 (2019) 212–223.
[153] Z. Zhang, A. Simon, C. Abetz, M. Held, A.-L. Höhme, E.S. Schneider, T. Segal-Peretz, V. Abetz, Hybrid organic–inorganic–organic isoporous membranes with tunable pore sizes and functionalities, for molecular separation 33 (2021), 2105251.
[154] J.E. Mondloch, W. Bury, D. Fairen-Jimenez, S. Kwon, E.J. DeMarco, M.H. Weston, A.A. Sarjeant, S.T. Nguyen, P.C. Stair, R.Q. Snurr, O.K. Farha, J.T. Hupp, Vapor-phase metalation by atomic layer deposition in a metal–organic framework, J. Am. Chem. Soc. 135 (2013) 10294–10297.
[155] L. Brožová, R. Zazpe, M. Otmar, J. Přikryl, R. Bulánek, J. Žitka, S. Krejčíková, P. Izák, J.M. Macak, Chiral templating of polycarbonate membranes by pinene using the modified atomic layer deposition approach, Langmuir 36 (2020) 12723–12734.
[156] X. Liang, D.M. King, M.D. Groner, J.H. Blackson, J.D. Harris, S.M. George, A. W. Weimer, Barrier properties of polymer/alumina nanocomposite membranes fabricated by atomic layer deposition, J. Membr. Sci. 322 (2008) 105–112.
[157] R.Z. Waldman, H.-C. Yang, D.J. Mandia, P.F. Nealey, J.W. Elam, S.B. Darling, Janus membranes via diffusion-controlled atomic layer deposition, Adv. Mater. Interfac. 5 (2018), 1800658.